



# The *abal/abaR* Quorum Sensing System Effects on Pathogenicity in *Acinetobacter baumannii*

Xiaoyu Sun<sup>1</sup>, Zhaohui Ni<sup>1</sup>, Jie Tang<sup>1</sup>, Yue Ding<sup>1</sup>, Xinlei Wang<sup>2</sup> and Fan Li<sup>1,3,4,5,6\*</sup>

<sup>1</sup> Department of Pathogenobiology, The Key Laboratory of Zoonosis, Chinese Ministry of Education, College of Basic Medicine, Jilin University, Changchun, China, <sup>2</sup> Department of Clinical Laboratory, The Second Hospital of Jilin University, Changchun, China, <sup>3</sup> The Key Laboratory for Bionics Engineering, Ministry of Education, Jilin University, Changchun, China, <sup>4</sup> Engineering Research Center for Medical Biomaterials of Jilin Province, Jilin University, Changchun, China, <sup>5</sup> Key Laboratory for Biomedical Materials of Jilin Province, Jilin University, Changchun, China, <sup>6</sup> State Key Laboratory of Pathogenesis, Prevention and Treatment of High Incidence Diseases in Central Asia, Xinjiang, China

## OPEN ACCESS

### Edited by:

Ilana Kolodkin-Gal,  
Weizmann Institute of Science, Israel

### Reviewed by:

Celia Mayer,  
University of Nottingham,  
United Kingdom  
Sunil D. Saroj,  
Symbiosis International University,  
India

### \*Correspondence:

Fan Li  
lifan@jlu.edu.cn

### Specialty section:

This article was submitted to  
Microbial Physiology and Metabolism,  
a section of the journal  
Frontiers in Microbiology

**Received:** 11 March 2021

**Accepted:** 08 June 2021

**Published:** 12 July 2021

### Citation:

Sun X, Ni Z, Tang J, Ding Y,  
Wang X and Li F (2021) The  
*abal/abaR* Quorum Sensing System  
Effects on Pathogenicity  
in *Acinetobacter baumannii*.  
*Front. Microbiol.* 12:679241.  
doi: 10.3389/fmicb.2021.679241

*Acinetobacter baumannii* is a Gram-negative pathogen that has emerged as one of the most troublesome pathogens for healthcare institutions globally. Bacterial quorum sensing (QS) is a process of cell-to-cell communication that relies on the production, secretion, and detection of autoinducer (AI) signals to share information about cell density and regulate gene expression accordingly. The molecular and genetic bases of *A. baumannii* virulence remains poorly understood. Therefore, the contribution of the *abal/abaR* QS system to growth characteristics, morphology, biofilm formation, resistance, motility, and virulence of *A. baumannii* was studied in detail. RNA sequencing (RNA-seq) analysis indicated that genes involved in various aspects of energy production and conversion; valine, leucine, and isoleucine degradation; and lipid transport and metabolism are associated with bacterial pathogenicity. Our work provides a new insight into the *abal/abaR* QS system effects on pathogenicity in *A. baumannii*. We propose that targeting the acyl homoserine lactone (AHL) synthase enzyme *abal* could provide an effective strategy for attenuating virulence. On the contrary, interdicting the AI synthase receptor *abaR* elicits unpredictable consequences, which may lead to enhanced bacterial virulence.

**Keywords:** *A. baumannii*, quorum sensing, *abal/abaR*, virulence, transcriptome

## INTRODUCTION

*Acinetobacter baumannii* is a Gram-negative, clinically important, opportunistic pathogen that causes a wide range of clinical infections. *A. baumannii* infections are increasingly difficult to treat because of multidrug resistance in most strains causing infection in intensive care units (ICUs) (Wong et al., 2017). Virulence factors were used by bacteria to enable successful interaction with and subsequent adhesion to and invasion of the human host (Harding et al., 2018). Previous studies have emphasized the importance of iron acquisition, transports, cell-associated pili, lipopolysaccharides, and outer membrane proteins such as *ompA*, *omp33*, and *surA1* for virulence (Smani et al., 2013; Liu et al., 2016; Vila-Farres et al., 2017), but studies of quorum sensing (QS) effects on pathogenicity in *A. baumannii* are limited. Bacterial QS is a process of cell-to-cell communication that relies on the production, secretion, and detection of autoinducer (AI) signals to share information about cell

density and regulate gene expression accordingly (Rutherford and Bassler, 2012). AIs are involved in the regulation of varied biological functions, including expression of virulence gene in *Vibrio cholerae* (Herzog et al., 2019), *Pseudomonas aeruginosa* PAO1 (Li et al., 2017), *Staphylococcus aureus* (Kim M.K. et al., 2017), *Escherichia coli* (Zuo et al., 2019), and other bacteria (Miller and Bassler, 2001).

*Acinetobacter baumannii* presenting a typical QS system (*abaI/abaR*) has been described (Bhargava et al., 2010). The *abaI* gene encodes 183 amino acids, and this protein was predicted to function in signal transduction. The *abaR* gene encodes 238 amino acids, and this protein is an AI synthase receptor (Bhargava et al., 2010). Previous studies on *A. baumannii* had focused on the role of QS systems in drug resistance, biofilm formation, and motility (Bhargava et al., 2015; Dou et al., 2017), but studies of QS effects on pathogenicity in *A. baumannii* are poor.

In this study, we used *A. baumannii* strain ATCC 17978, which has been the most frequently used model for scientific studies over the past two decades (Harding et al., 2018). A previous study isolated and characterized the AI synthase *abaI* from *A. baumannii* M2 but failed to create an *abaR* deletion mutant for unknown reasons (Niu et al., 2008). To explore the role of the *abaI/abaR* QS system in drug resistance, biofilm formation, and virulence of *A. baumannii*,  $\Delta$ *abaI*, and  $\Delta$ *abaR* mutants of strain ATCC 17978 were created. We also made double-mutant  $\Delta$ *abaIR*. The transcriptomes of wild type (WT),  $\Delta$ *abaI*,  $\Delta$ *abaR*, and  $\Delta$ *abaIR* were determined by RNA sequencing (RNA-seq).

## MATERIALS AND METHODS

### Bacterial Strains, Plasmids, and Culture Conditions

Bacterial strains and plasmids used in this study are listed in **Table 1**. *A. baumannii* strains were grown in lysogeny broth (LB). Antibiotics were used at the different concentrations for *E. coli* (kanamycin, 10 mg/L; ampicillin 25  $\mu$ g/ml; and tellurite, 6 mg/L) and for *A. baumannii* (tellurite, 30 mg/L; and tetracycline, 50 mg/L).

### Strain Construction

Strains  $\Delta$ *abaI*,  $\Delta$ *abaR*, and  $\Delta$ *abaIR* were unmarked deletion mutants created by a previous described method for acquiring markerless deletions in *A. baumannii* with minor modifications (Amin et al., 2013). The primers used in this study are listed in **Table 2**. Briefly, the upstream and downstream homologous arms of the target gene were amplified and fused and then ligated into a tellurite-resistant suicide vector with the T4 ligase, pMO130-Tel<sup>R</sup> (a generous gift from Addgene). The plasmid constructs were first introduced into *E. coli* DH5 $\alpha$  and subsequently selected on LB agar containing 30  $\mu$ g/ml kanamycin. The kanamycin-resistant colonies which carry an insertion of pMO130-Tel<sup>R</sup> and a 2-kb amplicon corresponding to the size of the ligated upstream and downstream homologous arms of the target gene were tested by the corresponding designed primers.

**TABLE 1** | Bacterial strains and plasmids used in this study.

Strain or plasmid	Relevant characteristics	Reference or source
<b><i>Acinetobacter baumannii</i> strains</b>		
ATCC 17978 (WT)		Ayush Kumar
$\Delta$ <i>abaI</i>	WT with deletion in <i>abaI</i> gene	This study
$\Delta$ <i>abaR</i>	WT with deletion in <i>abaR</i> gene	This study
$\Delta$ <i>abaIR</i>	WT with deletion in <i>abaI</i> and <i>abaR</i> genes	This study
$\Delta$ <i>abaI</i> (pME <i>abaI</i> )	$\Delta$ <i>abaI</i> harboring pME6032, containing the <i>abaI</i> gene	This study
$\Delta$ <i>abaR</i> (pME <i>abaR</i> )	$\Delta$ <i>abaR</i> harboring pME6032, containing the <i>abaR</i> gene	This study
WT(pME6032)	WT harboring pME6032, empty vector	This study
WT(pME <i>abaI</i> )	WT harboring pME6032, containing the <i>abaI</i> gene	This study
WT(pME <i>abaR</i> )	WT harboring pME6032, containing the <i>abaR</i> gene	This study
<b><i>E. coli</i> strains</b>		
DH5 $\alpha$	F- $\phi$ 80 <i>lacZ</i> $\Delta$ M15 $\Delta$ ( <i>lacZYA-argF</i> ) U169 A1 <i>recA1 hsdR17</i> ( <i>rk</i> -, <i>mk</i> +) <i>supE44</i> $\lambda$ - <i>thi-1 gyrA96 relA1 phoA</i>	TransGen
S17-1 (ATCC 47055)	Genotype: <i>recA pro hsdR RP4-2-Tc:Mu-Km:Tn7,Gm<sup>S</sup></i>	Biobw
<b><i>Chromobacterium violaceum</i></b>		
CV026	Detection of C4- and C6-HSLs	Mingsheng Dong
<b><i>Agrobacterium tumefaciens</i></b>		
KYC55 (pJZ372) (pJZ384) (pJZ410)	Detection of broad range of AHLs	Mingyong Zeng
R10 (pCF218)	<i>Ptet-traR</i> , Tc <sup>R</sup> , high AHL production strain	Mingyong Zeng
<b>Plasmids</b>		
pMO130-Tel <sup>R</sup>	Suicide plasmid, <i>xyI</i> E <sup>+</sup> , <i>sacB</i> <sup>+</sup> , <i>Km</i> <sup>R</sup>	Addgene
pMO130-Tel <sup>R</sup> - <i>abaI</i> -(Up/Down)	pMO130-Tel <sup>R</sup> containing a 1 kb UP fragment ( <i>abaI</i> ) and 1 kb DOWN fragment ( <i>abaI</i> )	This study
pMO130-Tel <sup>R</sup> - <i>abaR</i> -(Up/Down)	pMO130-Tel <sup>R</sup> containing a 1 kb UP fragment ( <i>abaR</i> ) and 1 kb DOWN fragment ( <i>abaR</i> )	This study
pME6032	Shuttle plasmid for genetic complementation, Tc <sup>R</sup>	Ke Lei Biological Technology Co., Ltd.
pME <i>abaI</i>	pME6032 containing the <i>abaI</i> gene (promoter and coding region)	This study
pME <i>abaR</i>	pME6032 containing the <i>abaR</i> gene (promoter and coding region)	This study

The resulting plasmids were used to transform into *E. coli* S17-1 and subsequently conjugate into *A. baumannii* ATCC 17978 via biparental conjugation. Exconjugants were selected on LB containing 30  $\mu$ g/ml tellurite and 25  $\mu$ g/ml ampicillin. *A. baumannii* ATCC 17978 harboring the inserted pMO130-Tel<sup>R</sup>-Gene-(Up/Down) construct was cultured in LB containing 10% sucrose and passed 7 days to select for stabilized deletion

**TABLE 2** | Primers used in this study.

Primer name	Sequence	Product
<i>abaR</i> ( <i>SphI</i> )up-F	TATGCATGCTTACGCCACTGACTAAGAG	1,190 bp
<i>abaR</i> ( <i>Bam</i> HI)up-R	GCTGGATCCCGATAAGAGACCACTAACCT	
<i>abaR</i> ( <i>Bam</i> HI)dw-F	TATGGATCCTTGAAGCGTAGGTCTAATCT	1,136 bp
<i>abaR</i> ( <i>Pst</i> I)dw-R	TATCTGCAGAAGGCGGTAAGTCTAAGAA	
<i>abal</i> ( <i>Pst</i> I)dw-F	TATCTGCAGCGCAACTACAGCCATACT	932 bp
<i>abal</i> ( <i>Not</i> I)dw-R	TATGCGGCCGCGCCTCTTACCGACTTACG	
<i>abal</i> -F	AAAGTTACCGCTACAGGG	435 bp
<i>abal</i> -R	CACGATGGGCACGAAA	
<i>abaR</i> -F	TCCTCGGGTCCCAATA	310 bp
<i>abaR</i> -R	TAAATCTACCGCATCAA	
<i>abal</i> ( <i>Eco</i> RI)-F	CCGGAATTCGGGTGGAAGCACTTGTAAATGAA	654 bp
<i>abal</i> ( <i>Xho</i> I)-R	CCGCTCGAGCGGCTCATCTTGCTCGGTCATA	
<i>abaR</i> ( <i>Eco</i> RI)-F	CCGGAATTCGGGTACAAAAGCCCTAGCATT	808 bp
<i>abaR</i> ( <i>Xho</i> I)-R	CCGCTCGAGCGGAAGATTAGACCTACGCTTCA	
pME6032-F	CCTCATCAGTGCCAACATA	843 bp
pME6032-R	CATACTCTGCGACATCGTA	

of gene and loss of the *sacB* gene by a second crossover and allelic replacement. If the target gene has been deleted, the PCR of genomic DNA from these bacteria would not produce any amplicon using a primer pair that anneals to the DNA that has been deleted. Mutants were complemented with the pME*abal* and pME*abaR* plasmids, generated by cloning the *abal* and *abaR* genes and ligation into a shuttle plasmid vector with the T4 ligase, pME6032 (Heeb et al., 2000). Overexpressed strains were transformed by the pME*abal* and pME*abaR* plasmids. The complemented strains and overexpressed strains were confirmed by PCR and restriction analysis of plasmids extracted from *A. baumannii* cells grown in LB medium containing 50 µg/ml tetracycline. All operations were performed in the P2 Laboratory of Basic Medical College of Jilin University, following the biosafety standard operating procedures of the Basic Medical College of Jilin University.

## Growth Curve Measurement

A single colony of strain was inoculated into 2 ml of LB and cultured with shaking (200 rpm) overnight at 37°C. The bacteria were collected by centrifugation at 4,000 rpm for 5 min and suspended in sterile saline to a turbidity comparable to a 0.5 McFarland standard. Twenty microliters was pipetted into a 96-well microtiter plate containing 180 µl of LB and incubated at 37°C. The optical density (OD)<sub>600</sub> of cultures was measured at hourly intervals for up to 48 h to draw the growth curve. Tests were performed on eight individual biological replicates, in triplicates.

## Transmission Electron Microscopy

Bacterial cells (OD<sub>450</sub> of 1.0) for SEM observation were harvested by centrifugation and washed three times with ddH<sub>2</sub>O. Bacteria were prefixed with 2.5% glutaraldehyde in 0.1 M phosphate buffer (pH 7.4). Images were captured at 120 kv with a HITACHI H-7650 transmission electron microscopy (TEM).

## Antimicrobial Susceptibility

*Acinetobacter baumannii* strains were cultured in LB liquid medium at 37°C with overnight shaking. Minimum inhibitory concentrations (MICs) for kanamycin, penicillin, streptomycin, meropenem, imipenem, ceftizoxime, cefepime, cefoperazone-sulbactam, piperacillin-tazobactam, ampicillin, tetracycline, and spectinomycin were determined on 96-well plates by the broth microdilution protocols of the Clinical and Laboratory Standards Institute, and the results of MIC testing were interpreted according to the criteria of the CLSI 2013 guidelines. All experiments were carried out a minimum of three times.

## Screening of Acyl Homoserine Lactone by *Chromobacterium violaceum* CV026 and *Agrobacterium tumefaciens* KYC55

*Acinetobacter baumannii* can produce acyl homoserine lactone (AHL) signal molecules with different chain lengths (Erdonmez et al., 2017); it is essential to use biosensors that detect a broad range of AHLs. *C. violaceum* CV026 specific for short-chain AHLs (C4–C6 AHL molecules) and *A. tumefaciens* KYC55 specific for long-chain AHLs (C8–C14 AHL molecules) were utilized for screening AHLs producing bacterial strains. By the presence of short-chain AHLs, CV026 produces purple pigments. By the presence of long-chain AHLs, a green color is observed for *A. tumefaciens* KYC55 (Erdonmez et al., 2017). Screening of the *A. baumannii* for production AHLs was carried out by agar plate diffusion assay with minor modifications (Lade et al., 2014; Erdonmez et al., 2017). Briefly, QS reporter strains were cultured in LB agar plates containing the antibiotics kanamycin 20 µg/ml for *C. violaceum* CV026 and spectinomycin 50 µg/ml and tetracycline 4.5 µg/ml for *A. tumefaciens* KYC55. The plates were incubated at 28°C for 24 h. As a visualizing agent, 40 µg/ml of X-gal was incorporated into the LB medium used for *A. tumefaciens* KYC55. For determining the production of acyl homoserine signal molecules, *A. baumannii* and mutants and biosensor *C. violaceum* CV026 and *A. tumefaciens* KYC55 strain were inoculated side by side such that they had a 0.5-cm gap between them. *C. violaceum* CV026 and *A. tumefaciens* KYC55 were assessed to be positive or negative according to the color changes in biosensor strain.

## Surface Motility Assay

The motility test was performed according to the method described previously with minor modifications (Clemmer et al., 2011). Briefly, the medium used for surface motility assay was tryptone broth [10 g/L tryptone (OXOID) and 5 g/L NaCl] supplemented with 0.3% (wt/vol) Noble agar (BD). Plates were prepared and inoculated with bacteria from an overnight culture in LB agar (1.5%, wt/vol) plates at 37°C with a sterile toothpick. All assays were carried out in triplicate in a minimum of three independent experiments. After incubation at 30°C for 12–14 h, the zone of motility at the agar/Petri dish interface was observed.

## Crystal Violet Biofilm Assay

The biofilm-forming ability test was performed in accordance with the method described previously with minor modifications

(Kaplan et al., 2012). Briefly, a few single colonies were suspended in sterile saline to a turbidity comparable to a 0.5 McFarland standard. The suspension was under vortex movement for 1 min; 20  $\mu$ l was pipetted into a 96-well microtiter plate containing 180  $\mu$ l of LB and incubated for 24 h at 37°C. For crystal violet staining, the wells were rinsed with phosphate-buffered saline (PBS) to exclude loosely adherent cells and then stained for 30 min with 200  $\mu$ l of 1% crystal violet. The wells were then rinsed with water and dried at room temperature. The amount of biofilm was quantitated by destaining the wells with 200  $\mu$ l of 33% acetic acid and then measuring the OD of the solution in a microplate spectrophotometer set at 595 nm. Tests were performed on 10 individual biological replicates, in triplicates. The differences between parent and mutant strains were calculated, and values returning a *P*-value of < 0.05 from Student's *t*-test were taken as significant.

### Serum Bactericidal Assay

The serum resistance experiment was performed in accordance with the method previously described with minor modifications (Harris et al., 2013). Briefly, 100  $\mu$ l mid-log-phase *A. baumannii* culture (a bacterial titer of approximately  $1 \times 10^5$  CFU) was mixed with 900  $\mu$ l of either normal human serum (NHS) or heat-inactivated serum (heated at 56°C for 30 min). The mixtures were incubated at 37°C, and aliquots of 100  $\mu$ l were removed from the culture at 1 h for the determination of bacterial counts. The number of surviving CFUs was determined by plating in triplicate. The results were expressed as percentage of survival, with 100% being the number of viable bacteria grown on brain heart infusion agar plates.

### Virulence in *Galleria mellonella*

*Galleria mellonella* has been known as a good model system to study *A. baumannii* pathogenesis (Peleg et al., 2009). The survival of ATCC 17978 and mutants in *G. mellonella* was measured as previously described (Peleg et al., 2009). An inoculum of  $10^6$  CFU bacteria was injected into *G. mellonella* larvae. After injection, the larvae were incubated at 37°C in darkness, and death was assessed at 24-h intervals over 7 days. The experiment was performed on 10 individual biological replicates, in triplicate. Statistical analysis was carried out with GraphPad Prism 6 to produce Kaplan–Meier survival curves. The statistical significance of differences between parent and  $\Delta$ *abaI*,  $\Delta$ *abaR*, and  $\Delta$ *abaIR* mutant strain survival curves was calculated with a log rank test. *P*-values of < 0.05 were considered significant.

### Murine Model of Pneumonia

Eight- to 10-week-old BALB/C mice were obtained from Jilin University. Mice were kept in a sterile environment at Jilin University and maintained according to standard procedures. All research was conducted in compliance with the institutional guidelines. The principles in the ARRIVE guidelines and the Basel declaration<sup>1</sup> have been considered when planning the experiments. Models of pulmonary infection were performed as previously described (Geisinger and Isberg, 2015).

<sup>1</sup><http://www.basel.declaration.org>

Briefly, infections were initiated by intraperitoneal injection of approximately  $1.2 \times 10^8$  CFU of bacteria suspended in 100  $\mu$ l of PBS into groups of mice (10 mice per group for survival studies; 5 per group for analyses of bacterial counts).

### Quantitative Bacteriology

To assess bacterial burden, the lung and spleen were aseptically operated and homogenized in 1 ml of sterile PBS using tissue homogenizers. Cultured on brain heart infusion agar plates were 100  $\mu$ l of the homogenates to quantify the bacterial load of *A. baumannii* in the respective organs.

### RNA-Seq and Analysis

RNA was extracted from three biological replicates of each strain with a GeneMark Total RNA Purification Kit. RNA libraries were prepared and sequenced with Illumina HiSeq 2000 at the Beijing Genomics Institute (BGI). Sequences were mapped onto the ATCC 17978 genome (accession no. cp018664.1) using Bowtie 2. Differentially expressed genes (DEGs) were identified using the DESeq2 package (Bioconductor). Genes were deemed as differentially expressed if they presented a log<sub>2</sub>-fold change greater than 1 or less than  $-1$  and if *P*-value (*P*-adj) was less than 0.05 in the mutant strain compared to the WT strain. Cluster of orthologous groups (COG) enrichment analysis was performed by dividing the percentage of genes upregulated or downregulated for each category by the percentage of genes in that category across the whole genome (Tatusov et al., 2000; Galperin et al., 2015). MultiExperiment Viewer version 4.9.0 was used to perform hierarchical clustering and heat map visualization (Howe et al., 2011). Gene Ontology (GO) and Kyoto Encyclopedia of Genes and Genomes (KEGG) pathway enrichment analyses, based on R software, were applied for the identification of pathways in which DEGs were significantly enriched. The GO and KEGG pathway analyses of the DEGs were conducted through the clusterProfiler package in R software (Yu et al., 2012). A *P*-value of < 0.05 was considered to have statistical significance and to achieve significant enrichment. Quantitative reverse transcription (qRT)-PCR was performed on the 7300 Plus Real-Time PCR System (Applied Biosystems) using a standard protocol from the FastStart Universal SYBR Green Master (Roche, Basel, Switzerland). Gene expression levels were quantified by using the  $2^{-\Delta \Delta C_t}$  method with endogenous controls (16S). The primers used for qRT-PCR assays are described in Table 3. All qRT-PCR assays were repeated 3 $\times$ . The RNA-seq data obtained in this study were submitted to GEO, with accession number GSE173396.

## RESULTS

### The Mutants Showed Differences in Growth Characteristics and Morphology

To test the role of the *abaI/abaR* QS system in the *A. baumannii* growth curve, we determined the OD of the culture over time. The growth of the  $\Delta$ *abaR* and  $\Delta$ *abaIR* mutants did not differ from that of the parent strain (Figure 1A). The

**TABLE 3** | Real-time quantitative PCR primers.

qRT-PCR	Sequence
AUO97_RS01130-F	CGCAACGCCATTACTA
AUO97_RS01130-R	TTGTTTATCGCATTCTG
AUO97_RS01135-F	TTGCTCCACCCACATA
AUO97_RS01135-R	TTGGCGTAACCTCACTT
AUO97_RS08710-F	ATGCCGAGTTTGCTTA
AUO97_RS08710-R	AACACGCTGTGAATCTTT
AUO97_RS13835-F	CGGTGCTTGATGTGCT
AUO97_RS13835-R	AAATGCGATAACGTGGA
AUO97_RS17125-F	GTCTACGCCGCTCTGT
AUO97_RS17125-R	AGGTTATTGAAGTGGG
AUO97_RS17130-F	CCACATACGCCCTTGCT
AUO97_RS17130-R	CCTCGGGAGATTCATT
AUO97_RS17135-F	TTTTGGGCATACTGACTTT
AUO97_RS17135-R	CCTCTGGACTCGGTAATGT
AUO97_RS17140-F	CCTTTGGTGCCGTAGA
AUO97_RS17140-R	ACCCGAACCTCACAGAC
AUO97_RS17145-F	GCGTTCCCAAGCCTCA
AUO97_RS17145-R	CTCGGTGATTACGATGGATG
AUO97_RS17160-F	CACCCAACCCACTGAA
AUO97_RS17160-R	AGCGTATGTGAGCCAAG
16S_qF	CAGCTCGTGTGATGATGT
16S_qR	CGTAAGGGCCATGATGACTT

complemented strain  $\Delta abaR$  (pME $abaR$ ) and overexpressed strains WT(pME $abaI$ ) and WT(pME $abaR$ ) also showed growth profiles similar to those of the WT (**Figure 1A**), suggesting that the gene  $abaR$  is not essential for *A. baumannii* growth. In contrast, the  $\Delta abaI$  mutant showed visibly slowed growth at the logarithmic phase. The growth of the  $\Delta abaI$  mutant was partly rescued by the expression of  $abaI$  via the pME6032-derived plasmid pME $abaI$  (**Figure 1A**). The empty vector pME6032, used as a control, did not affect the growth profile of *A. baumannii* ATCC 17978 (**Figure 1A**). These results demonstrated that  $abaI$  affects the growth of *A. baumannii*. Subsequently, the morphology of the bacteria was observed by TEM. As shown in **Figure 1B**, WT was attached with extracellular secretions.  $\Delta abaI$  mutant cell edges were transparent. The  $\Delta abaR$  mutant strain's cytoplasmic density is lower. There was no obvious change in the  $\Delta abaIR$  mutant, but around the cell adhered partial secretions. The morphology of the  $\Delta abaI$  mutant was partly rescued by the expression of  $abaI$  via the plasmid pME $abaI$ . The morphology of the  $\Delta abaR$  mutant was rescued by the expression of  $abaR$  via the plasmid pME $abaR$ . There was no significant difference between WT and the overexpressed strain WT(pME $abaI$ ). The overexpressed strain WT(pME $abaR$ ) attached a large number of extracellular secretions. The empty vector pME6032, used as a control, did not affect the morphology of *A. baumannii* ATCC 17978. These results indicated that  $abaI$  is closely related to cell morphology and extracellular secretions.

### Mutants Showed Increased Susceptibility to Antimicrobials

To determine whether deletion of QS genes changed in the drug resistance, the MICs of commonly used antibiotics for

strains were determined. There was a decrease in the MICs of kanamycin, gentamicin, penicillin, streptomycin, meropenem, imipenem, and ampicillin for QS gene deletions compared to WT. Drug susceptibility of  $\Delta abaI$  and  $\Delta abaR$  mutants was partly rescued by expressions of  $abaI$  and  $abaR$  via plasmids pME $abaI$  and pME $abaR$ , respectively. The overexpressed strain WT(pME $abaI$ ) was more resistant in cefepime and cefoperazone-sulbactam. WT(pME $abaR$ ) was more resistant in kanamycin, streptomycin, ceftizoxime, cefepime, cefoperazone-sulbactam, and piperacillin-tazobactam. The empty vector pME6032, used as a control, partly affects the drug susceptibility of *A. baumannii* ATCC 17978 (**Table 4**). These results indicated that QS affects antimicrobial sensitivity. The preliminary research of the research group showed that  $abaI$  and  $abaR$  genes positively correlated with bacterial resistance rates (Tang et al., 2020).

### Screening of Strains for AHL Production

To detect the effect of the QS system on AHL of the strains, two different biosensor strains were used. As a result, no strains were found to produce AHLs based on the development of purple coloration in the CV026 reporter strain (**Figures 2A–C**).  $\Delta abaI$ ,  $\Delta abaR$ , and  $\Delta abaIR$  were not observed to produce AHLs based on the development of green coloration in the *A. tumefaciens* KYC55 reporter strain. AHL production of  $\Delta abaI$  and  $\Delta abaR$  mutants was rescued by expressions of  $abaI$  and  $abaR$  via plasmids pME $abaI$  and pME $abaR$ , respectively. The empty vector pME6032, used as a control, did not affect the AHL production of *A. baumannii* ATCC 17978 (**Figures 2D–F**). These results indicate that both  $abaI$  and  $abaR$  can affect AHL production and that *A. baumannii* may produce only long-chain signal molecules, not short-chain AHLs.

### Surface-Associated Motility Relies on QS

To explore the role of QS in motility, we tested these strains' surface motility phenotype on LB medium supplemented with 0.3% agar. As a result,  $\Delta abaI$ ,  $\Delta abaR$ , and  $\Delta abaIR$  mutants compared with WT strain showed no obvious motility, motility of  $\Delta abaI$  mutants was not rescued by the expression of  $abaI$  via the plasmid pME $abaI$ , and motility of  $\Delta abaR$  mutants was partly rescued by the expression of  $abaR$  via the plasmid pME $abaR$ . The empty vector pME6032, used as a control, has an inhibitory effect on the motility of *A. baumannii* ATCC 17978. The overexpressed strain WT(pME $abaR$ ) compared with the WT strain showed significantly increased motility. There was no significant difference between the overexpressed strain WT(pME $abaI$ ) and WT in the motility (**Figures 3A,B**). These results indicated that the QS system affects the motility of bacteria and that the effect of  $abaR$  is stronger than that of the  $abaI$  mutant on motility, since the  $\Delta abaI$ (pME $abaI$ ) could not rescue the normal phenotype in comparison with  $\Delta abaR$ (pME $abaR$ ) (**Figure 3A**).

### Biofilm Formation

To investigate the role of QS in biofilm formation on an abiotic surface, we cultivated the strain mutants in 96-well plates for 24 h at 37°C. As a result, filaments were formed in the culture medium of the WT strain, mutant strains  $\Delta abaI$  and  $\Delta abaR$

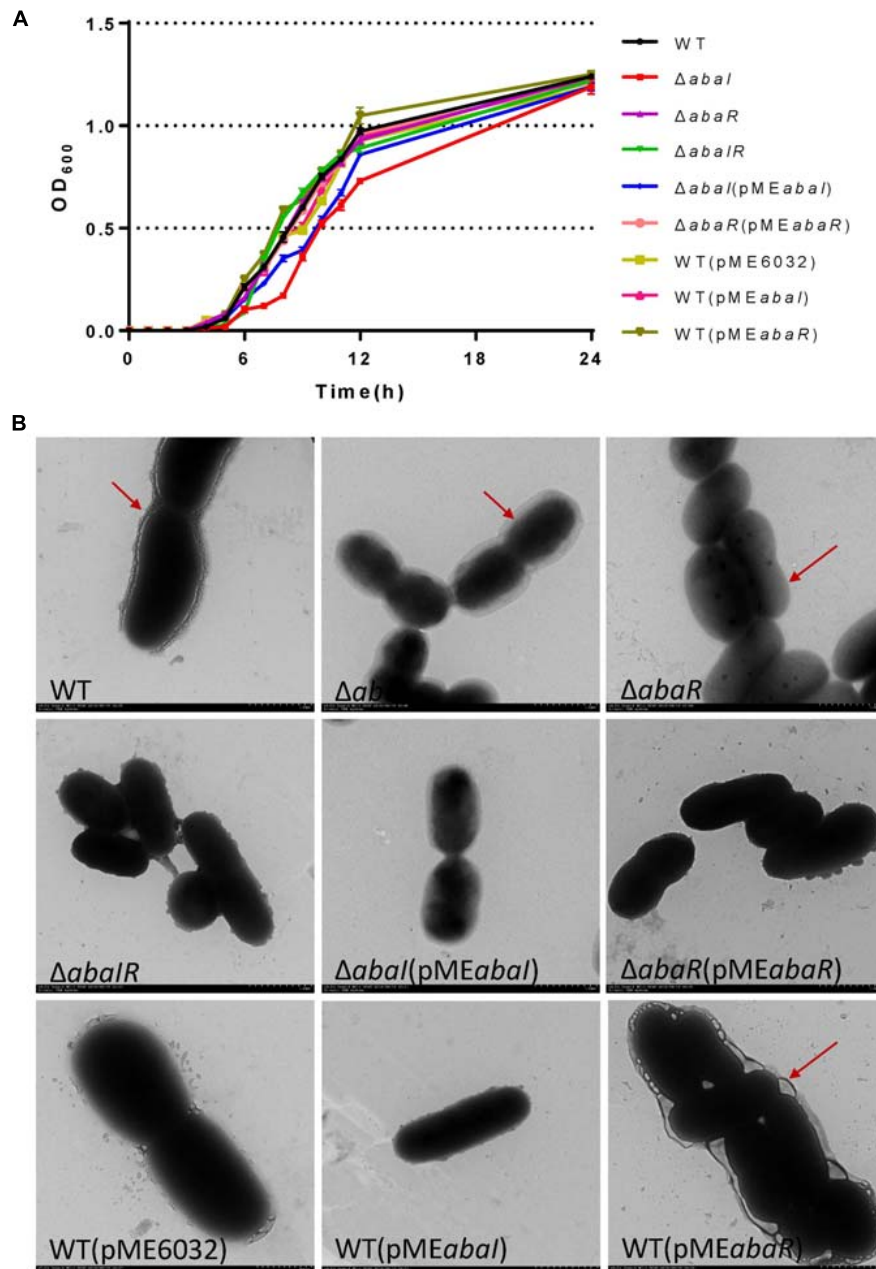


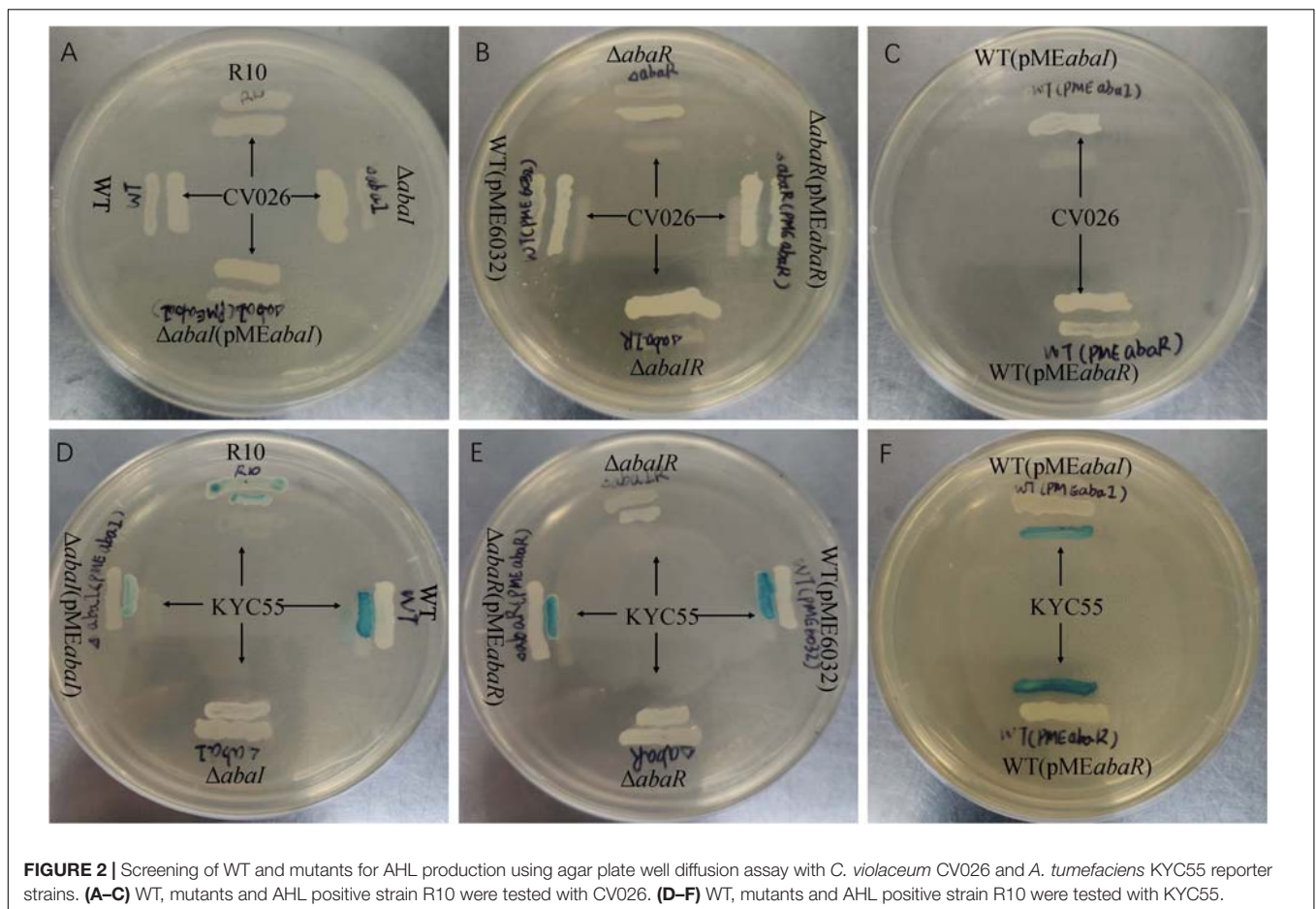
**FIGURE 1 | (A)** Growth curve analysis of *A. baumannii* and mutants in broth. **(B)** TEM images of the targeted bacteria. Cells were observed with a HITACHI H-7650 TEM operated at 120 kV. Scale bar = 500 nm.

had dot-like biofilm formation on the surface of liquid, the  $\Delta abaIR$  mutant strain had no biofilm on the liquid surface, there were dot-like biofilms on the liquid surface of  $\Delta abaI(pMEabaI)$  and  $\Delta abaR(pMEabaR)$ , and they were connected into pieces. The biofilm on the liquid surface of the overexpressed strain WT(pMEabaI) was lamellar, while the biofilm on the liquid surface of WT(pMEabaR) was spot-like but thick (Figure 4A). The membrane at the liquid–gas interface of the WT(pME6032) was not obvious. The absorbance of the bacterial solution was detected, and the results are shown in Figure 4B; there

were significant differences between the absorbance of the parental strain and mutants  $\Delta abaI$  and  $\Delta abaR$ ; however, the mutant  $\Delta abaIR$  showed no difference. The absorbance of  $\Delta abaI$  mutants was not rescued by the expression of *abaI* via the plasmid pMEabaI, and the absorbance of  $\Delta abaR$  mutants was rescued by the expression of *abaR* via the plasmid pMEabaR. The absorbance of the overexpressed strain WT(pMEabaR) was significantly higher than that of the WT strain and WT(pME6032). The biofilm-forming ability of the strains was determined by crystal violet biofilm assay, and the differences

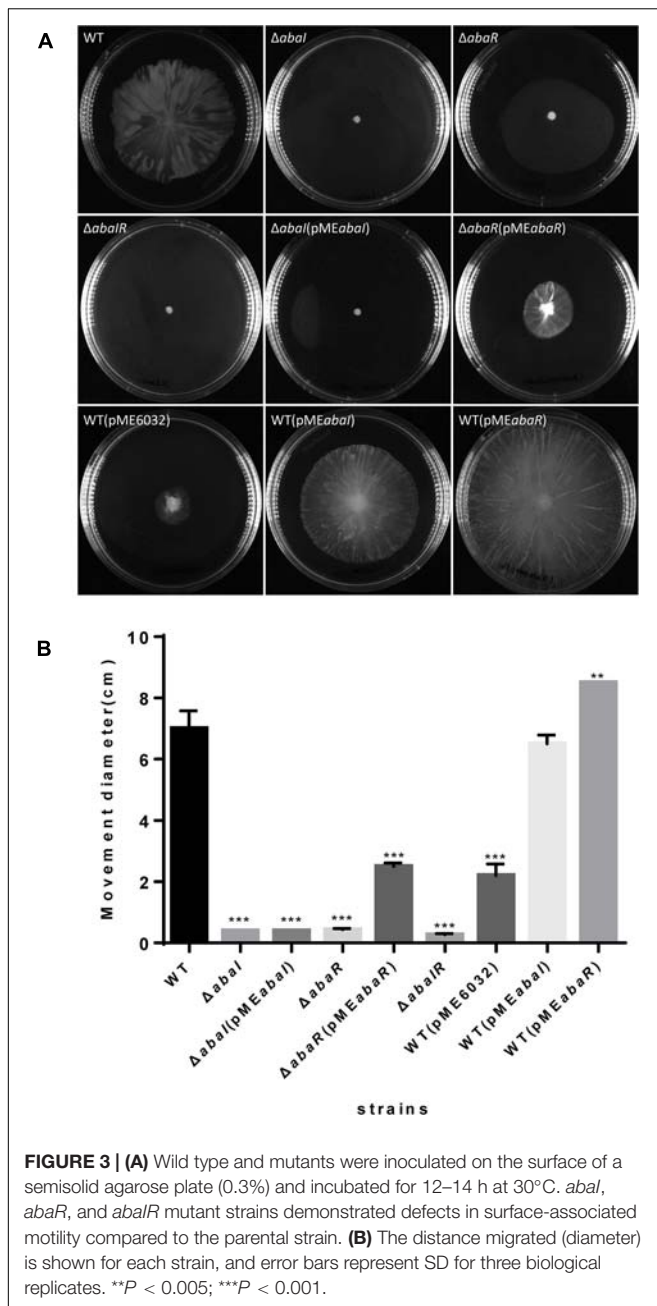
**TABLE 4** | Minimum inhibitory concentrations of antibiotics used in this study.

Antibiotic	MIC ( $\mu\text{g/ml}$ )								
	WT	$\Delta abal$	$\Delta abar$	$\Delta abalR$	$\Delta abal(\text{pME}abal)$	$\Delta abar(\text{pME}abar)$	WT(pME6032)	WT(pME $abal$ )	WT(pME $abar$ )
Kanamycin	8	2	4	4	4	8	8	8	16
Gentamicin	4	1	4	0.25	2	4	4	4	4
Penicillin	128	64	64	32	64	64	64	64	128
Streptomycin	32	16	16	16	32	32	32	32	64
Meropenem	1	0.25	0.5	0.25	0.5	0.5	1	1	1
Imipenem	32	16	16	8	16	16	16	16	32
Ceftizoxime	8	8	8	8	8	8	8	8	16
Cefepime	2	8	8	2	8	8	8	8	8
Cefoperazone–sulbactam	2	8	2	2	8	4	2	4	4
Piperacillin–tazobactam	8	8	8	32	8	8	8	8	16
Vancomycin	>512	>512	128	>512	>512	>512	>512	>512	>512
Ampicillin	64	32	64	32	32	32	32	32	64
Tetracycline	2	8	2	2	8	4	4	4	4
Spectinomycin	64	64	64	64	64	64	64	64	64



between the WT and mutant strains were calculated. Compared with that of WT strains, the biofilm formation of all strains was significantly decreased, except for that of the overexpressed strain WT(pME $abar$ ), which was significantly higher than that of the WT strain (Figure 4C). WT(pME $abal$ ) produced less biofilm

in comparison with its control WT(pME6032) harboring the plasmid alone, which may be due to the influence of plasmid pME $abal$  on the secretion of some proteins in the WT strain. The results indicated that QS system affects the pellicle biofilm formation in the liquid–air interface.



## Serum Killing

Serum sensitivity has been involved in the toxic mechanisms of *A. baumannii*; to elucidate the virulence of strains, we compared the serum sensitivity of strains to NHS. As shown in **Figure 5A**, WT, *abaR*, and WT(pMEabaR) survived after incubation in serum, whereas  $\Delta abaI$ ,  $\Delta abaI(pMEabaI)$ , and  $\Delta abaIR$  were entirely killed after 1 h at 37°C. The serum sensitivity of  $\Delta abaI$  mutants was not rescued by the expression of *abaI* via the plasmid pMEabaI, and the serum sensitivity of  $\Delta abaR$  mutants was rescued by the expression of *abaR* via the plasmid pMEabaR. The empty vector pME6032, used as a control, did not affect the serum sensitivity of *A. baumannii* ATCC 17978. These results

indicated that WT and  $\Delta abaR$  were highly resistant to the serum; in contrast,  $\Delta abaI$  and  $\Delta abaIR$  mutants were much more serum sensitive, showing a significant difference ( $P < 0.001$ ).

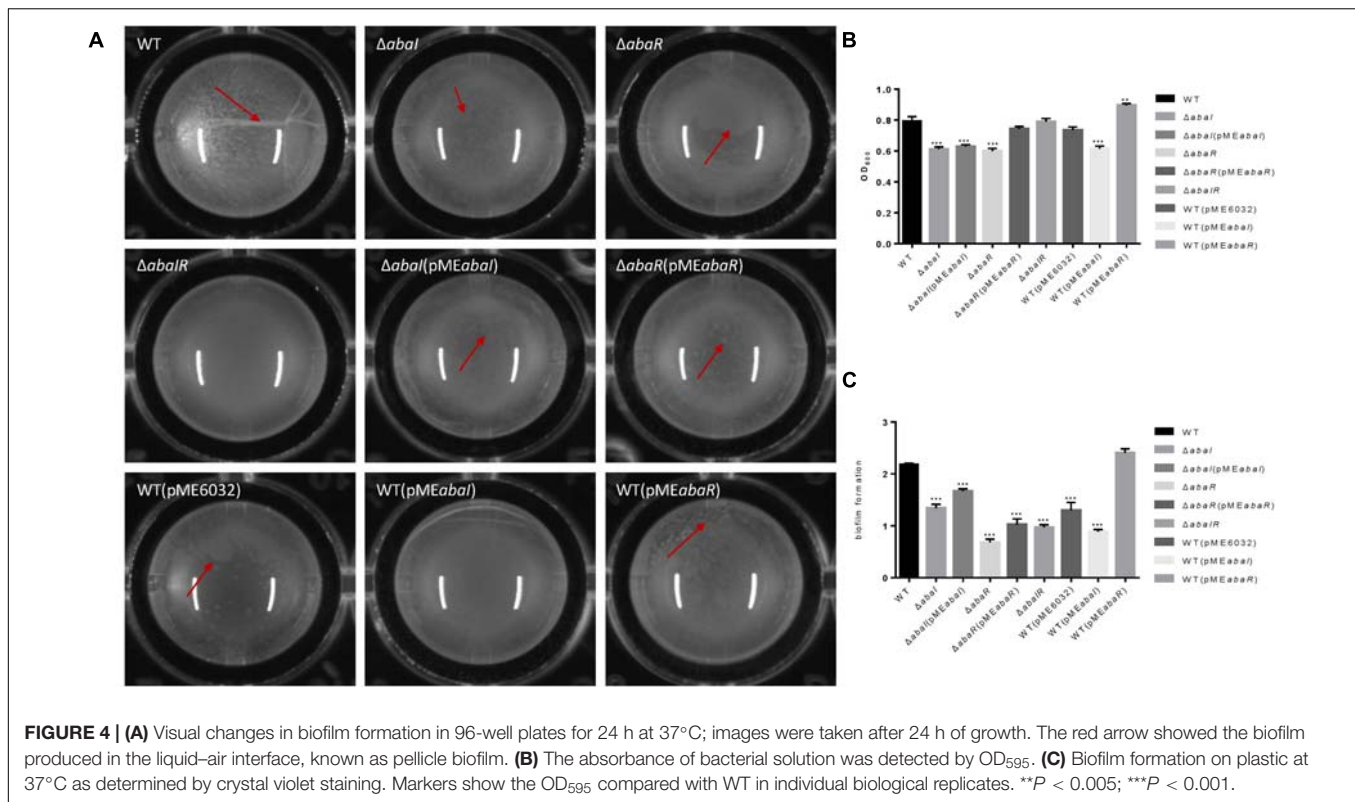
## QS Plays a Role in Virulence in *G. mellonella* Infection Models

Quorum sensing controls the production of virulence factors in many bacterial species and is regarded as an attractive target to combat bacterial pathogenicity (Mukherjee et al., 2018). To explore whether QS genes are an important virulence factor determinant for *A. baumannii* in *G. mellonella*, we assessed the virulence of the QS mutant strains compared to the isogenic parent strain ATCC 17978.  $\Delta abaI$  and  $\Delta abaIR$  mutants were completely avirulent in this assay, and the  $\Delta abaIR$  mutant was slightly more pathogenic than the  $\Delta abaI$  mutants but less pathogenic than the  $\Delta abaR$  mutants, while the  $\Delta abaR$  mutant remained fully virulent, killing *G. mellonella* larvae as toxic as the WT (**Figure 5B**). Consistent with this finding, Laura Fernandez-Garcia et al. (2018) found that injection of *G. mellonella* larvae with the *A. baumannii* ATCC 17978 strain caused higher mortality than injection with the mutant *A. baumannii* ATCC 17978  $\Delta abaI$ . The virulence of the  $\Delta abaI$  mutant was not rescued by the expression of *abaI* via the plasmid pMEabaI, and the virulence of the  $\Delta abaR$  mutant was not rescued by the expression of *abaR* via the plasmid pMEabaR. The empty vector pME6032, used as a control, reduced the virulence of *A. baumannii* ATCC 17978. The virulence of the overexpressed strains WT(pMEabaI) and WT(pMEabaR) was significantly reduced compared to that of the parent strain ATCC 17978 (**Figure 5B**). The virulence of strains WT(pMEabaI) and WT(pMEabaR) was not significantly different from that of WT(pME6032). The results indicated that the QS system plays a role in virulence in *G. mellonella* infection models and that plasmids not only affect the virulence of WT strains but also affect the virulence of complement strains.

## QS Plays a Role in Virulence in Mouse Infection Models

Whether these QS genes of *A. baumannii* are important for virulence to a mammalian system is currently unknown. To evaluate the virulence of strains, we established a bacteremia model in mice by intraperitoneal injection of *A. baumannii*. In the experiments, we analyzed the survival of infected mice with this model and found that a dose of approximately  $1.8 \times 10^8$  CFU of  $\Delta abaI$  and  $\Delta abaIR$  mutants was unable to cause lethality, but only one mouse (10 per group) survived in the WT group, and all the mice in the  $\Delta abaR$  group died (date not shown) after 48 h. Subsequently, we used a dose of approximately  $1.2 \times 10^8$  CFU of bacteria to infect 10 mice per group for survival studies. We observed that  $\Delta abaI$  and  $\Delta abaIR$  mutants were unable to cause lethality; WT exhibited a low fatality rate, but  $\Delta abaR$  complemented with strain  $\Delta abaR(pMEabaR)$  can cause more deaths (**Figure 6A**). To explore the virulence of mutants in host resistance against *A. baumannii* infection, the blood, lungs, and spleens from BALB/C mice were collected at various time points after being injected with  $1.2 \times 10^8$  CFU of *A. baumannii*. We analyzed bacterial burdens in the blood, lung, and spleen of mice





infected for 4, 24, and 72 h. As a result, the WT and  $\Delta abaR$  mutant complemented with strain  $\Delta abaR(pMEabaR)$  resulted in an increase in bacterial counts, and  $\Delta abaI$  and  $\Delta abaIR$  mutants exhibited a remarkable reduction in the burden in blood, lung, and spleen at 4 h post inoculation. More specifically, as shown,  $\Delta abaI$  and  $\Delta abaIR$  mutants displayed a high serum clearance rate, resulting in a significant decrease in bacteremia at 4 h post inoculation. There were no differences at 24 h (Figure 6B). The bacteria were completely eliminated at 72 h (data not shown). These results indicated that deletion of *abaI* results in weaker toxicity in mouse models, while deletion of *abaR* results in enhanced virulence.

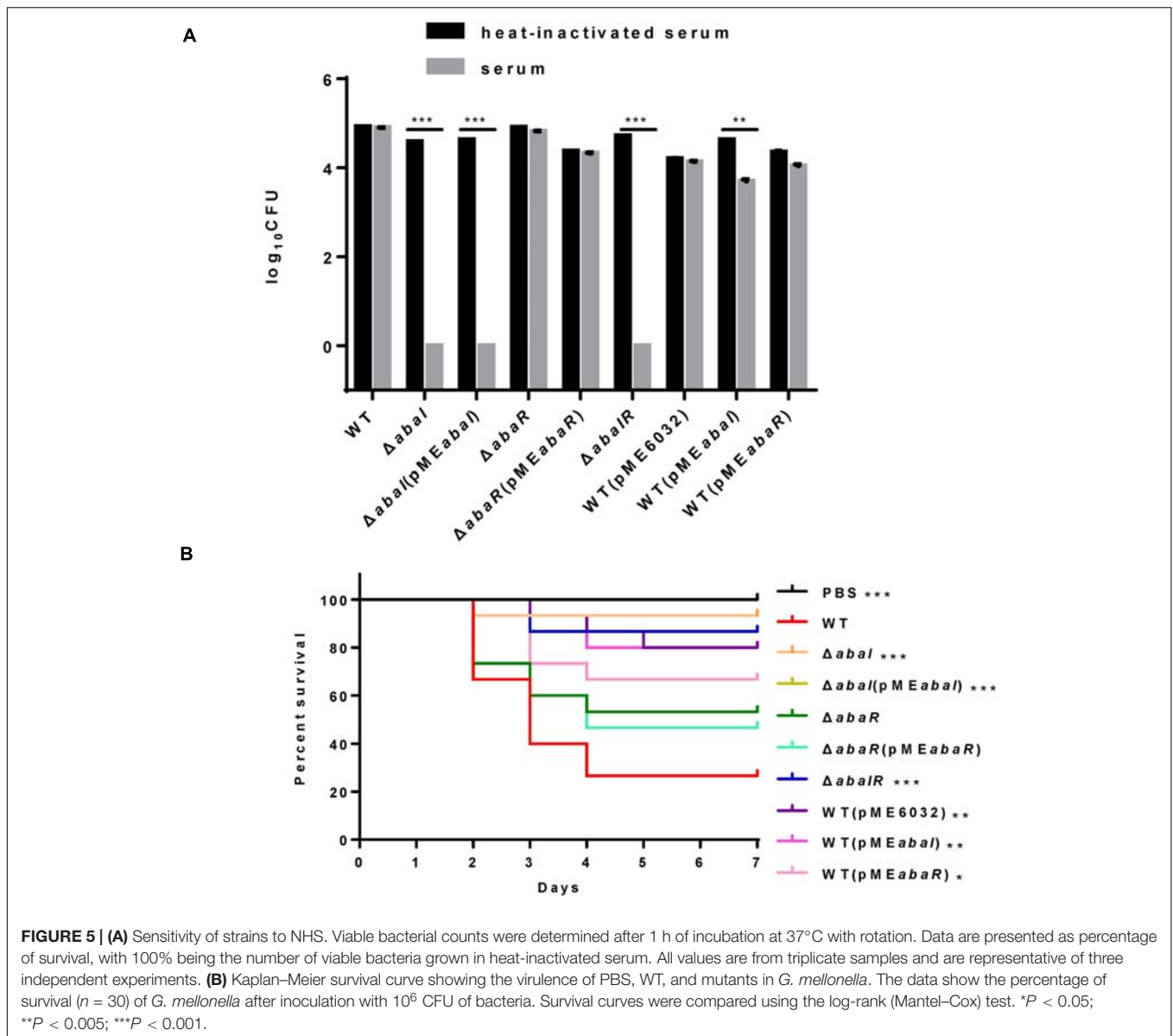
### Mutants Cause Differential Gene Expression in *A. baumannii* ATCC 17978

To identify transcriptional activity dependent on *abaI/abaR* function, RNA-seq analysis was performed on *abaI/abaR* mutants and the WT strain. A total of 463 genes were classified as differentially expressed in mutants relative to WT. Compared with that in WT, in the  $\Delta abaI$  mutant, a total of 159 protein-coding genes (out of 3,848) were identified as differentially expressed by a log<sub>2</sub>-fold change greater than 1 or less than -1 ( $P \leq 0.05$ ) (126 with increased expression and 33 with decreased expression). Deletion of *abaR* had a larger impact on the transcriptome of strain ATCC 17978, with the differential expression of 324 genes (211 upregulated and 113 downregulated). The  $\Delta abaIR$  mutant had a total of 123 DEGs (79 genes with increased expression and 44 with decreased

expression) (Figures 7A–C and Supplementary Tables 1–3). These results revealed that partial changes in gene expression occur with changes in *abaI/abaR*. To validate our RNA-seq analysis, qRT-PCR was used to validate the 10 upregulated genes (Figure 7D). The results were consistent with the high-throughput sequencing data.

Given the different phenotypes of  $\Delta abaI$ ,  $\Delta abaR$ , and  $\Delta abaIR$  mutants, the RNA-seq analysis revealed a subset of the genes that was most highly activated or suppressed by the QS system, as shown in Figure 7B. We centralized our analysis on the gene subsets whose transcription was down in  $\Delta abaI$ ,  $\Delta abaR$ , and  $\Delta abaIR$  mutants; the QS gene (*abaI* AUO97\_RS06645) and nearby locus (AUO97\_RS06600–06630) showed strongly reduced transcription. One study found that in the *A. baumannii* M2 strain, QS mediated by the *abaI* is required for motility (Clemmer et al., 2011). We assessed the surface motility of the mutants, as shown in Figure 3. We observed that the WT strain exhibited a robust surface motility phenotype and that the mutants did not exhibit any signs of motility.

We mainly analyzed the gene expression of each group. Hemerythrin-like proteins have an effect on oxidation-reduction regulation and antibiotic resistance (Li et al., 2015). AUO97\_RS11650 (hemerythrin) was downregulated in the  $\Delta abaI$  mutant, and other antimicrobial resistance genes including AUO97\_RS07490 (*mexK*), AUO97\_RS07485 (*mexJ*), AUO97\_RS07485 (efflux RND transporter periplasmic adaptor subunit), and AUO97\_RS05665 (beta-lactamase domain protein) were downregulated. One gene, AUO97\_RS16540 (*AdeA/AdeI* family multidrug efflux RND transporter periplasmic adaptor



subunit) had a 1.2-fold increased expression in the  $\Delta abal$  mutant, while the expression of this gene was not changed in the  $\Delta abalR$  mutant. We then assessed the antimicrobial susceptibility of the mutants, as shown in **Table 4**, and found that the susceptibility of mutants toward a part of antimicrobials increased.

The *csu* operon is composed of six genes (*csuA/BABCDE*) and plays a central role in initial bacterial attachment and biofilm formation on abiotic surfaces (Tomaras et al., 2003). In the  $\Delta abal$  mutant, the *CsuA/BABCDE* chaperone–usher pili assembly system showed a high expression, except for the *CsuA* (AUO97\_RS19210) gene. In the  $\Delta abar$  mutant, *CsuA/B* (AUO97\_RS19215), *CsuA* (AUO97\_RS19210), *CsuB* (AUO97\_RS19205), and *CsuC* (AUO97\_RS19200) were highly expressed, whereas in the  $\Delta abalR$  mutant, only *CsuA/B* (AUO97\_RS19215) was highly expressed. *CsuA/B* is predicted

to form part of the type I pili rod that was upregulated in all mutants (**Figure 7B**). Of particular interest is their regulator genes *bfmR–bfmS*, which did not change in all mutants. Biofilm formation was observed on the liquid surface of the  $\Delta abal$  and  $\Delta abar$  mutants (**Figure 4A**). A previous study found that *CsuC* and *CsuE* are required in the early steps of biofilm formation (Tomaras et al., 2003). In some *A. baumannii* strains, biofilms are not essential for virulence (Smith et al., 2007). Apart from the *csu* operon, other genes were controlled by QS, which may be related with biofilm formation. A1S\_0644 (AUO97\_RS08180), a hypothetical protein involved in biofilm formation, was repressed in the  $\Delta abar$  mutant.

Secreted bacterial proteins can mediate serum resistance; a secreted serine protease termed PKF is required for serum resistance and inhibits biofilm formation in *A. baumannii* (King et al., 2013). In the  $\Delta abar$  mutant, PKF (AUO97\_RS01525)

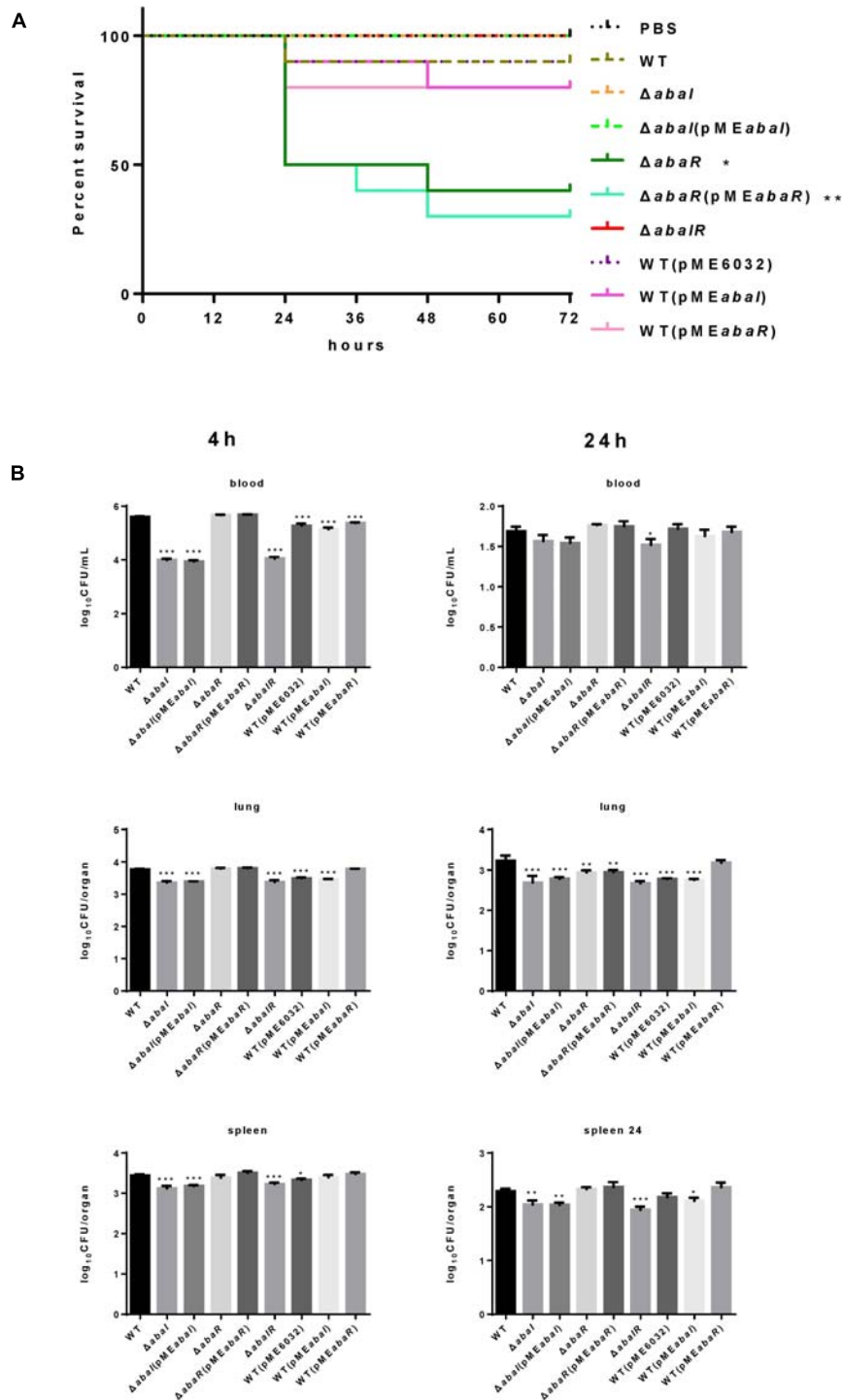
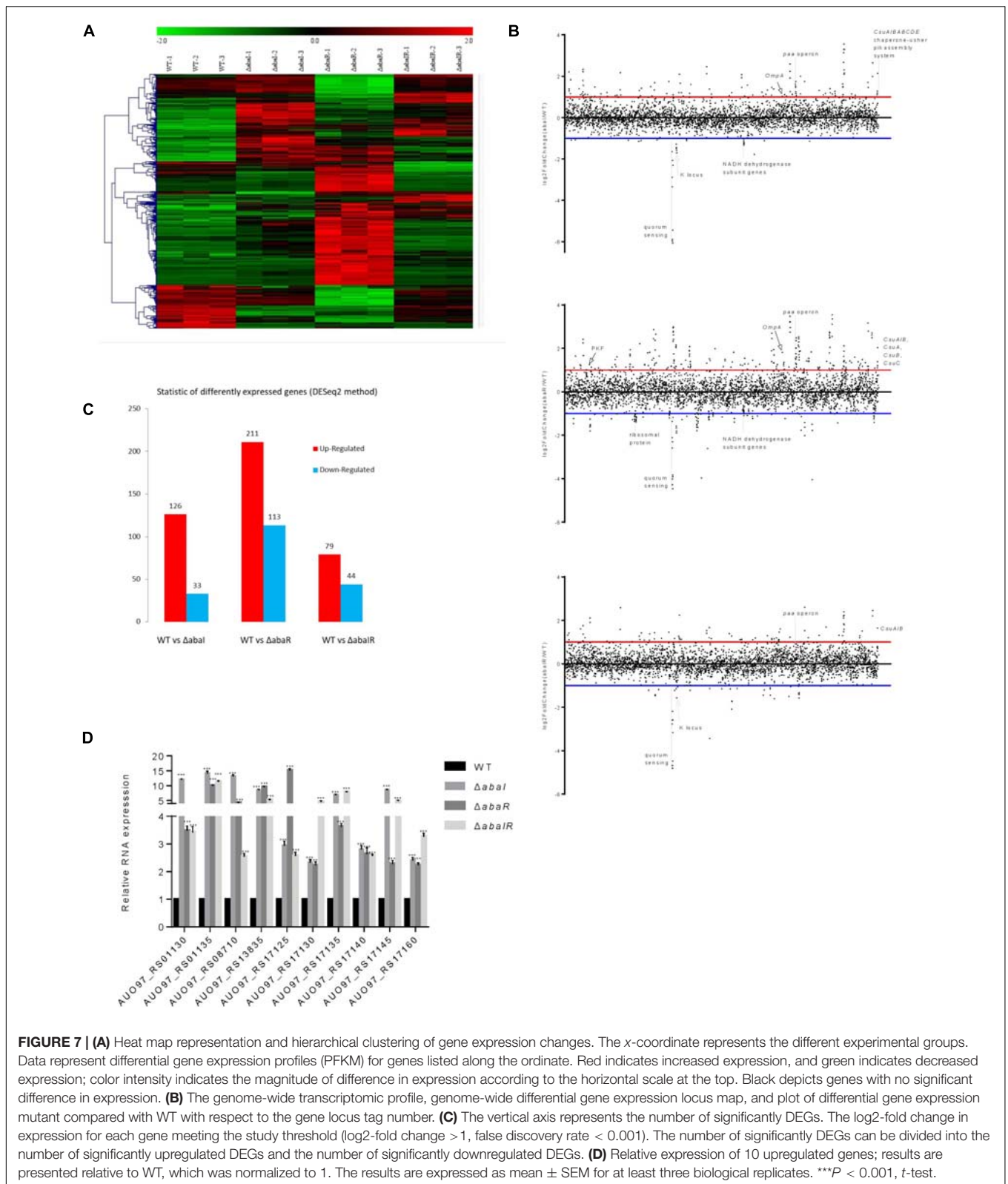


**FIGURE 6 | (A)** Kaplan–Meier survival curve of mouse inoculated with strains at a dose of  $1.2 \times 10^8$  CFUs ( $n = 10$ ). Survival curves were compared using the log-rank (Mantel–Cox) test,  $*P < 0.05$ ;  $**P < 0.005$ . **(B)** *A. baumannii* bacterial burdens in the lungs, spleen, and blood. Bacterial burdens in the blood and respective organs were determined by quantitative bacteriology at 4 and 24 h post inoculation. An unpaired *t*-test was used to validate the experimental data.  $*P < 0.05$ ;  $**P < 0.005$ ;  $***P < 0.001$ .

was highly expressed, and no difference was observed in the  $\Delta abaI$  and  $\Delta abaIR$  mutants (**Figure 7B**). We assessed the serum sensitivity test and the ability of mutants to form biofilms on

the abiotic surface. As shown in **Figures 4, 5A**, WT and  $\Delta abaR$  survived after incubation in serum, whereas  $\Delta abaI$  and  $\Delta abaIR$  were entirely killed after 1 h at 37°C. There was a remarkable



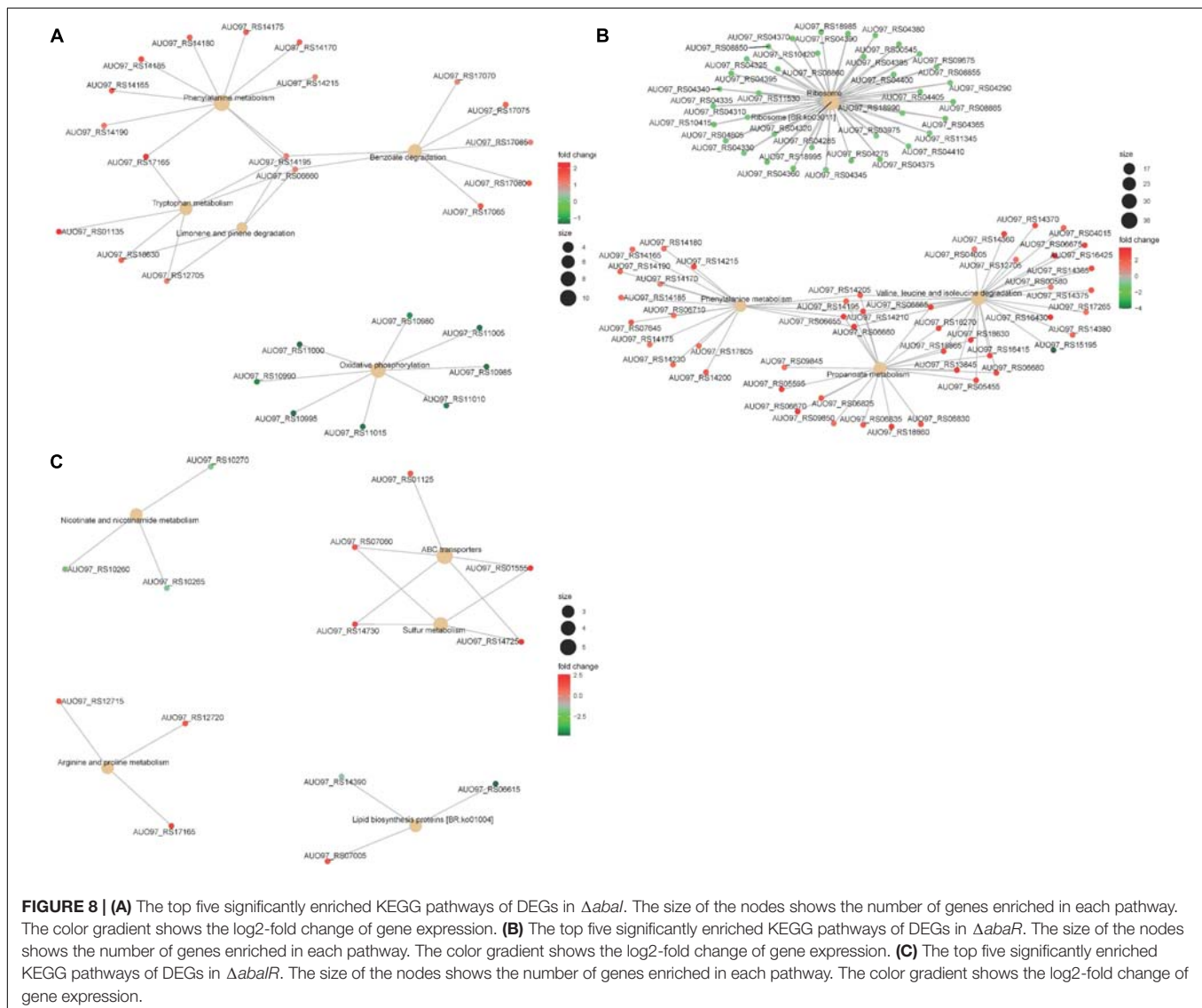
decrease in the biofilm formation by the  $\Delta$ abaR mutant. Apart from this gene, other genes that may be associated with serum resistance and biofilm formation may be regulated by QS.

NADH is mainly involved in material and energy metabolism in cells, which is transferring energy to ATP synthesis through oxidative phosphorylation on the mitochondrial inner

membrane (YanJun et al., 2019; Yu et al., 2019). In the respiratory chain of *A. baumannii*, there are 14 NADH-quinone oxidoreductase subunits involved in NADH dehydrogenase, which include *NuoA–NuoN*. In the  $\Delta abaI$  mutant, a subset of genes including AOU97\_RS10980–11015 (*NuoG*, *NuoH*, *NuoI*, *NuoJ*, *NuoK*, *NuoL*, *NuoM*, and *NuoN*) was all downregulated (Figure 8A). In the  $\Delta abaR$  mutant, AOU97\_RS11000 (*NuoK*) and AOU97\_RS11015 (*NuoN*) were downregulated, and there was no change in the  $\Delta abaIR$  mutant. One study found that these genes are essential in affecting growth in the LB medium (Wang et al., 2014). We then assessed the growth characteristics and morphology of the mutants, as shown in Figures 1A,B; the  $\Delta abaI$  mutant showed slightly slowed growth at the logarithmic phase, the cytoplasm of the  $\Delta abaI$  mutant appeared to be transparent, and the cytoplasmic density of the  $\Delta abaI$  mutant is relatively low. These genes play a significant role in mediating cell growth and energy metabolism in *A. baumannii*. Apart from NADH dehydrogenase, other genes that may be

associated with cell growth and energy metabolism may be regulated by QS. In the  $\Delta abaI$  mutant, a subset of genes involved in benzoate degradation (AOU97\_RS17065–17085) and tryptophan metabolism and limonene and pinene degradation was upregulated; this strain may utilize the beta-ketoadipate pathway and tryptophan for energy supply (Figure 8A).

The phenylacetic acid (PAA) catabolic pathway encoded by the *paa* operon is a key route in the catabolism of the Krebs cycle, and this pathway is thought to contribute to bacterial virulence (Teufel et al., 2010; Cerqueira et al., 2014). The cluster is composed of 15 coding sequences (*paaZ*, *paaA*, *paaB*, *paaC*, *paaD*, *paaE*, *paaF*, *paaG*, *paaH*, *paaI*, *paaK1*, *paaK2*, *paaX*, *paaY*, and *paaI*). In the  $\Delta abaR$  mutant, the *paa* operon was highly expressed (Figure 8B). In the  $\Delta abaI$  mutant, AOU97\_RS14165 (*paaZ*), AOU97\_RS14170 (*paaA*), AOU97\_RS14175 (*paaB*), AOU97\_RS14180 (*paaC*), AOU97\_RS14185 (*paaD*), AOU97\_RS14190 (*paaE*), AOU97\_RS14195 (*paaF*), and AOU97\_RS14215 (*paaK1*) were highly expressed (Figure 8A),



and the expression of this operon was not changed in the  $\Delta abaIR$  mutant.

Branched-chain amino acids (BCAAs), including leucine (Leu), isoleucine (Ile), and valine (Val), are vital to both growth and virulence in bacteria (Kaiser et al., 2016; Kim G.L. et al., 2017). In the  $\Delta abaR$  mutant, the Val, Leu, and Ile degradation pathways were upregulated (**Figure 8B**). The BCAAs serve as precursors for branched-chain fatty acids (BCFAs), which are predominant membrane fatty acids; the BCAAs are key co-regulators of virulence factors.

Propionate is one of the most abundant short-chain fatty acids (SCFAs). In bacteria, propionate catabolism plays an important role in virulence (Dolan et al., 2018). In the  $\Delta abaR$  mutant, there are 27 genes involved in the propanoate metabolism pathway that were upregulated (**Figure 8B**). In  $\Delta abaIR$  mutant, Nicotinate and nicotinamide metabolism and Lipid biosynthesis proteins are reduced. Sulfur metabolism and Arginine and proline metabolism were enhanced, which may contribute to the virulence of the strain (**Figure 8C**). We assessed the virulence of the mutant in *G. mellonella*. As shown in **Figure 5B**, the  $\Delta abaIR$  mutant enhances slightly more virulent than  $\Delta abaI$ . In the  $\Delta abaI$  mutant, AUO97\_RS14195, AUO97\_RS16430, AUO97\_RS06660, AUO97\_RS18630, and AUO97\_RS12705 involved in the propanoate metabolism pathway were upregulated. In the  $\Delta abaIR$  mutant, AUO97\_RS14380, AUO97\_RS14375, and AUO97\_RS14370 involved in the propanoate metabolism pathway were upregulated.

Lipids play an important role in both the physiology and pathophysiology of living systems (Pereira-Dutra et al., 2019). Membrane phospholipids play a key role in the defense against antimicrobials, including host fatty acids (Eijkelkamp et al., 2018; Beavers et al., 2019; Jiang et al., 2019). The COG enrichment analysis indicated that a large amount of genes with predicted functions in [I] lipid transport and metabolism (21%) was upregulated in the  $\Delta abaR$  mutant (**Figure 9**). PAAs, BCAAs, SCFAs, and lipid transport and metabolism may play a protective role against the host and serum.

The K locus regulates the production of complex polysaccharides to protect against killing by host serum and enhance virulence in animal models of infection (Geisinger and Isberg, 2015). In the K locus (O-glycosylation and wzy-dependent capsule synthesis locus) (AUO97\_RS06870–06965), the gene AUO97\_RS06875 (UDP-glucose 4-epimerase GalE) showed weakened transcription in the  $\Delta abaI$  and  $\Delta abaIR$  mutants by a 1.7-fold decrease and a 1.6-fold decrease, respectively, while there was no change in the  $\Delta abaR$  mutant (**Figure 7B**).

AUO97\_RS13365 (OMPA family protein), a naturally glycosylated protein in *A. baumannii* ATCC 17978, was expressed with a 1.8-fold increase in  $\Delta abaR$  strain, and no difference in  $\Delta abaI$  and  $\Delta abaIR$  mutants was observed (**Figure 7B**).

Ribosomal proteins (RPs) are well known for their role in mediating protein synthesis and maintaining the stability of the ribosomal complex, which includes small and large subunits. There were 36 genes encoding for RPs that exhibited reduced expression in the  $\Delta abaR$  mutant strain (**Figure 8B**). Twenty-three (L1–L6, L9–L13, L15–L20, L22–L23, L25, L28, L29, and L35) of them were associated with the large subunit while the

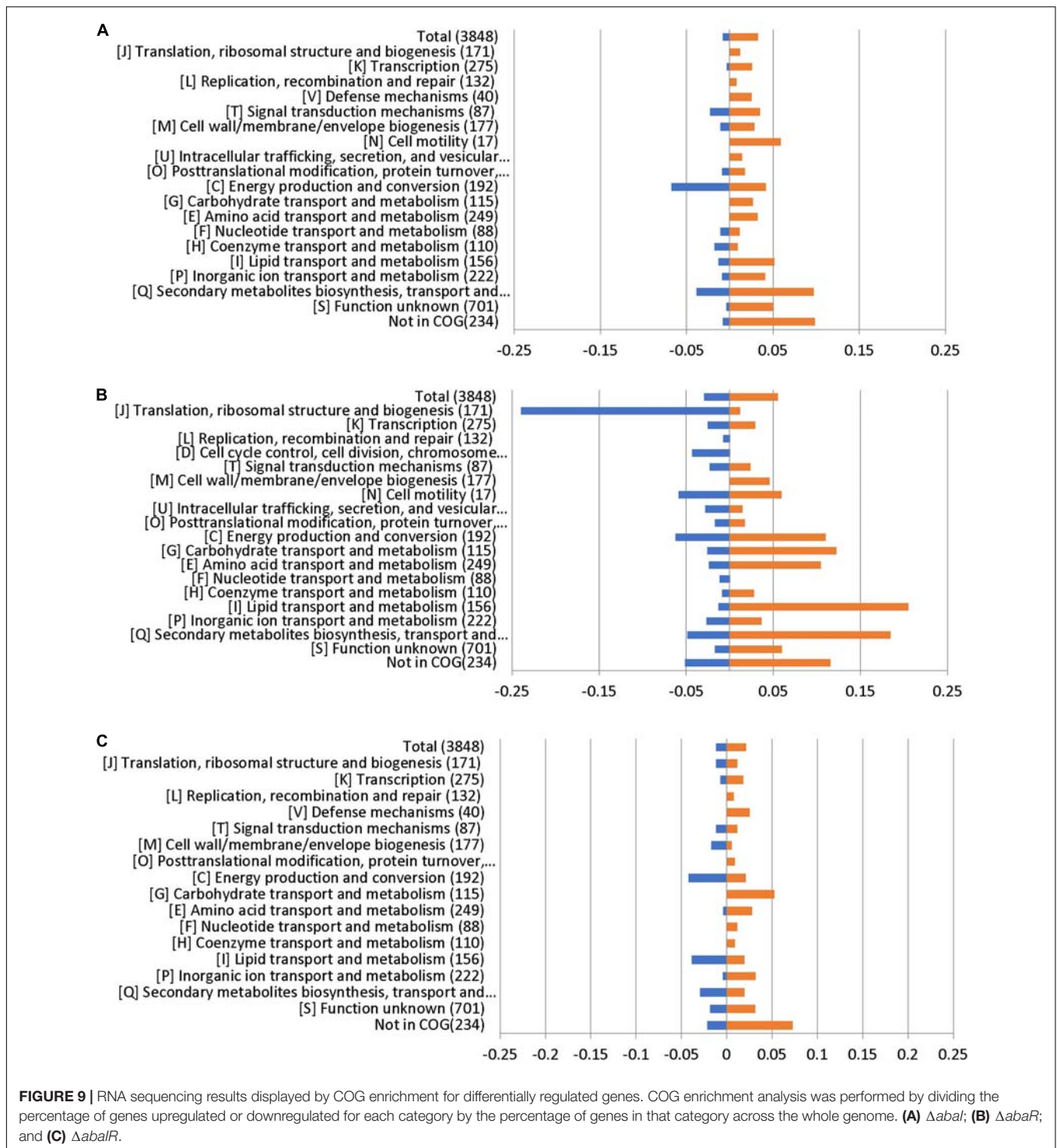
remaining 13 (S2–S8, S10, S11, S14, and S17–S19) were associated with the small subunit. This change may enable *A. baumannii* to “fine-tune” their proteomes to regulate the pathogenicity of bacteria. There was no change in  $\Delta abaI$  and  $\Delta abaIR$  mutants. We assessed the virulence of the mutant in *G. mellonella* and mouse and serum sensitivity tests. As shown in **Figures 5A,B, 6**, the  $\Delta abaR$  mutant enhances more virulence and serum resistance, while  $\Delta abaI$  and  $\Delta abaIR$  mutants markedly attenuated the virulence of *A. baumannii*. The selected genes (*paaG*, *paaH*, *paaJ*, *paaK2*, *paaX*, *paaY*, and *paaI*) encode proteins in the PAA catabolic pathway and BCAAs, and the capsule synthesis loci *GalE* and *OmpA* may contribute to virulence.

## COG Annotation

To link transcriptional reprogramming by *abaI/abaR* to function, DEGs were categorized into COGs (Tatusov et al., 2000; Huerta-Cepas et al., 2017). The COG enrichment analysis identified that 7% of the genes belonging to the COG category [C] energy production and conversion were significantly repressed and that 10% of the genes were associated with the COG category [Q] secondary metabolites biosynthesis, transport, and catabolism were highly regulated in the  $\Delta abaI$  mutant. We observed a high proportion of genes with increased expression in the  $\Delta abaR$  mutant that encoded proteins involved in [I] lipid transport and metabolism (21%); [Q] secondary metabolites biosynthesis, transport, and catabolism (18%); [G] carbohydrate transport and metabolism (12%); [C] energy production and conversion (11%); and [E] amino acid transport and metabolism (10%), while observing a strong decrease in [J] translation, ribosomal structure, and biogenesis (24%). In the  $\Delta abaIR$  mutant, 4% of the genes belonging to the COG category [C] energy production and conversion and [I] lipid transport and metabolism were downregulated, while 5% of the genes belonging to the COG category [G] carbohydrate transport and metabolism were upregulated (**Figure 9**).

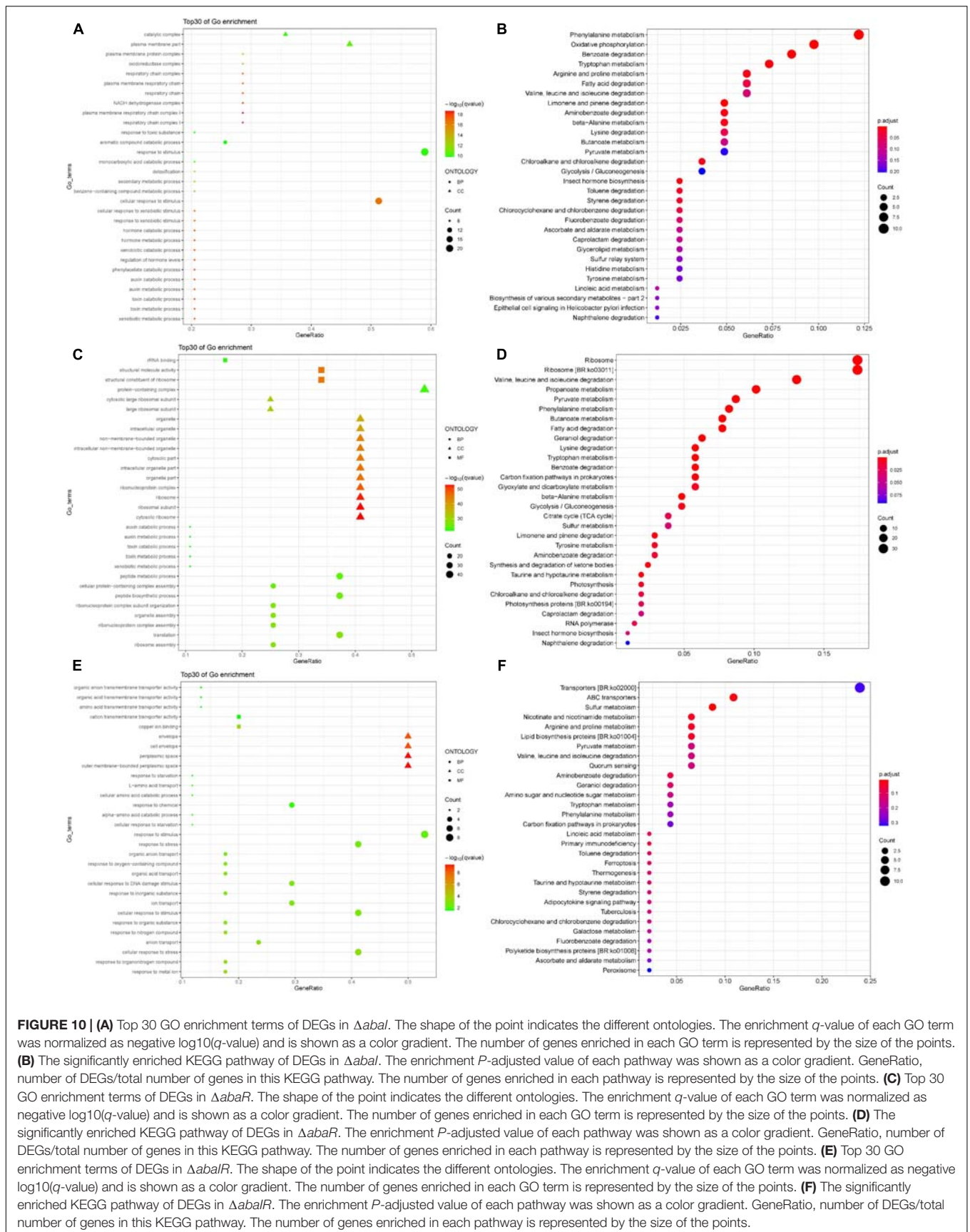
## GO and KEGG Pathway Enrichment Analyses of DEGs

The functions of the DEGs were annotated and classified based on GO and KEGG pathway enrichment analyses. The top 30 significant GO terms were divided into two major categories – biological process and cellular component in the  $\Delta abaI$  mutant – as shown in **Figure 10A**. Among the biological processes, DEGs were distributed to the xenobiotic metabolic process, toxin metabolic/catabolic process, auxin metabolic/catabolic process, phenylacetate catabolic process, and so on. In the cellular component field, DEGs belonged to respiratory chain complex I, plasma membrane respiratory chain complex I, NADH dehydrogenase complex, and respiratory chain. The top 30 significant GO terms were divided into three major categories – biological process, cellular component, and molecular function in  $\Delta abaR$  mutant – as shown in **Figure 10C**. Among the biological processes, DEGs were distributed to ribosome assembly, translation, ribonucleoprotein complex assembly, organelle assembly, ribonucleoprotein complex subunit organization, and peptide biosynthetic



process. In the cellular component field, DEGs belonged to cytosolic ribosome, ribosome, ribonucleoprotein complex, organelle part, and cytosolic part. In molecular function, DEGs were responsible for the structural constituent of ribosome, structural molecule activity, and rRNA binding. The top 30 significant GO terms were divided into three major categories – biological process, cellular component,

and molecular function in the  $\Delta$ abaIR mutant – as shown in **Figure 10E**. Among the biological processes, DEGs were distributed to response to metal ion, response to organonitrogen compound, cellular response to stress, and anion transport. In the cellular component field, DEGs belonged to the outer membrane-bounded periplasmic space, periplasmic space, cell envelope, and envelope. In molecular





function, DEGs were responsible for copper ion binding and cation/amino acid/organic acid/organic anion transmembrane transporter activity.

Kyoto Encyclopedia of Genes and Genomes pathway enrichment suggested that DEGs of the  $\Delta abaI$  mutant were significantly enriched in the pathways related to phenylalanine metabolism, oxidative phosphorylation, benzoate degradation, tryptophan metabolism, arginine and proline metabolism, fatty acid degradation, and so on (Figure 10B). DEGs of the  $\Delta abaR$  mutant were mainly involved in the pathways related to ribosome; Val, Leu, and Ile degradation; propanoate metabolism; pyruvate metabolism; phenylalanine metabolism; fatty acid degradation; and so on (Figure 10D). DEGs of the  $\Delta abaIR$  mutant were mainly involved in the pathways related to ABC transporters, sulfur metabolism, nicotinate and nicotinamide metabolism, and so on (Figure 10F).

## DISCUSSION

*Acinetobacter baumannii* has become a very important hospital-acquired pathogen. Bacterial virulence is the prime determinant for the deterioration of an infected patient's health. QS is a cell-to-cell communication system utilized by bacteria to promote collective behaviors. Many bacteria use QS to control virulence.

Our lab's previous research found that the *abaI/abaR* QS system was widely distributed among the *A. baumannii* clinical isolates, was necessary for surface-related motility, and was significantly correlated with drug resistance and virulence to *G. mellonella* (Tang et al., 2020). In the present study, we focused on detecting the role of the *abaI/abaR* QS system in the virulence of *A. baumannii* ATCC 17978. The mutant lacking *abaI* is believed to be less virulent than the WT strain. In contrast, the *abaR* mutants were significantly more pathogenic than the WT strain. This result was confirmed in our study by injection of *G. mellonella* larvae and a mouse model of infection and serum killing test. Our transcriptomic analysis results revealed that deletion of *abaI* leads to the significant repression of energy production and conversion genes. The connection between energy metabolism and virulence has been reported in a multitude of bacteria. In *V. cholerae*, the expression of virulence regulatory protein *ToxT* is affected by the NADH via respiration activity (Minato et al., 2013). In *Pseudomonas savastanoi*, *RhpR* directly regulates multiple metabolic pathways and phosphorylation to specifically control virulence (Xie et al., 2019). Therefore, *abaI* may indirectly control bacterial virulence by inducing the differential expression of some key genes involved in NADH dehydrogenase in the respiratory chain. Deletion of *abaR* enhances more cytotoxicity and immune evasion. RNA-seq analysis indicated that deletion of *abaR* leads to the significant overexpression of lipid transport and metabolism, carbohydrate transport and metabolism, and amino acid transport and metabolism genes. Lipid metabolism plays a key role in the pathogenicity of some intracellular bacteria (Rameshwaram et al., 2018). It has been observed that lipids are the main carbon and energy source of *Mycobacterium tuberculosis*, which switches from carbohydrate utilization to

the fatty acid utilization pathway for the establishment of a successful infection (Mukhopadhyay et al., 2012). *A. baumannii* is a ubiquitous, facultative intracellular bacterial pathogen (Tang et al., 2018). The  $\Delta abaR$  mutant may enhance lipid transport and metabolism to play a protective role against the host. The  $\Delta abaIR$  mutant was slightly more pathogenic than the  $\Delta abaI$  mutants but less pathogenic than the  $\Delta abaR$  mutants. This result was verified in our study by injection of bacteria into *G. mellonella* larvae.

Virulence through the intermediated phenylacetate catabolism pathway has been found in *A. baumannii*, and deletion of *paaE* attenuated *A. baumannii* virulence in the mouse septicemia model (Cerqueira et al., 2014). In *Burkholderia cenocepacia*, *paaA* and *paaE* insertional mutants showed reduced virulence, and interruption of *paaZ* and *paaF* slightly increased virulence in the *Caenorhabditis elegans* model of infection (Law et al., 2008). Therefore, deletion of the *abaR* gene may indirectly enhance bacterial virulence via triggering the differential expression of a lot of key genes involved in the phenylacetate catabolism pathway. The selected genes (*paaG*, *paaH*, *paaJ*, *paaK2*, *paaX*, *paaY*, and *paaI*) encode proteins in the PAA catabolic pathway that may contribute to virulence. *abaI* is a protein that synthesizes AHLs, and *abaR* is a LuxR homolog transcription factor/receptor for AHLs (Stacy et al., 2012). In this study, only the WT strain was observed to produce AHLs based on *A. tumefaciens* KYC55 reporter strains, while the green pigment was not observed in  $\Delta abaI$ ,  $\Delta abaR$ , and  $\Delta abaIR$  mutants. No purple pigment was observed in all strains based on *C. violaceum* CV026. In a previous study, the absence of purple pigment may be attributed to the low rate of production of short-chain homoserine lactone and fast degradation in the strains (Erdozmez et al., 2017). Our transcriptomic analysis results revealed that deletion of *abaR* leads to the significant repression of *abaI*. Therefore, *abaR* may be a repressor such that repression is relieved when AHLs are bound. The results suggest that *abaR* generally represses its regulon of genes until it binds AHLs. When AHLs are bound, then repression is relieved. This may explain why deletion of *abaI* is substantially different from deletion of *abaR*. When *abaI* is mutated, then *abaR* still represses the expression of many genes, such as those associated with virulence. When both genes were knocked out, the virulence of the strain was moderate to low level.

The present research will help advance the functional genomic analysis of the QS system in *A. baumannii* and provides a new insight into *abaI/abaR* QS system effects on pathogenicity in *A. baumannii*. We propose that targeting the AHL synthase enzyme *abaI* could provide an effective strategy for attenuating virulence. On the contrary, interdicting the AI synthase receptor *abaR* elicits unpredictable consequences, which may lead to enhanced bacterial virulence.

## DATA AVAILABILITY STATEMENT

The datasets presented in this study can be found in online repositories. The names of the repository/repositories and accession number(s) can be found in the article/Supplementary Material.

## ETHICS STATEMENT

The animal study was reviewed and approved by Experimental Animal Center, Jilin University. Written informed consent was obtained from the owners for the participation of their animals in this study.

## AUTHOR CONTRIBUTIONS

ZN and FL designed the experiments and revised the manuscript. XS performed the experiments, analyzed the data and wrote the manuscript. JT and YD performed the experiments. XW interpreted the data. All authors contributed to the article and approved the submitted version.

## FUNDING

This research was partially funded by grants from National Natural Science Foundation of China (81601817 and 81672109), Jilin Province Development and Reform Commission (2015Y031-5), Education Department of Jilin Province

## REFERENCES

- Amin, I. M., Richmond, G. E., Sen, P., Koh, T. H., Piddock, L. J., and Chua, K. L. (2013). A method for generating marker-less gene deletions in multidrug-resistant *Acinetobacter baumannii*. *BMC Microbiol.* 13:158. doi: 10.1186/1471-2180-13-158
- Beavers, W. N., Monteith, A. J., Amarnath, V., Mernaugh, R. L., Roberts, L. J., Chazin, W. J., et al. (2019). Arachidonic acid kills staphylococcus aureus through a lipid peroxidation mechanism. *mBio* 1, 10.
- Bhargava, N., Sharma, P., and Capalash, N. (2010). Quorum sensing in *Acinetobacter*: an emerging pathogen. *Crit. Rev. Microbiol.* 36, 349–360. doi: 10.3109/1040841x.2010.512269
- Bhargava, N., Singh, S. P., Sharma, A., Sharma, P., and Capalash, N. (2015). Attenuation of quorum sensing-mediated virulence of *Acinetobacter baumannii* by Glycyrrhiza glabra flavonoids. *Future Microbiol.* 10, 1953–1968. doi: 10.2217/fmb.15.107
- Cerqueira, G. M., Kostoulas, X., Khoo, C., Aibinu, I., Qu, Y., Traven, A., et al. (2014). A global virulence regulator in *Acinetobacter baumannii* and its control of the phenylacetic acid catabolic pathway. *J. Infect. Dis.* 1, 46–55. doi: 10.1093/infdis/jiu024
- Clemmer, K. M., Bonomo, R. A., and Rather, P. N. (2011). Genetic analysis of surface motility in *Acinetobacter baumannii*. *Microbiology* 157, 2534–2544. doi: 10.1099/mic.0.049791-0
- Dolan, S. K., Wijaya, A., Geddis, S. M., Spring, D. R., Silva-Rocha, R., and Welch, M. (2018). Loving the poison: the methylcitrate cycle and bacterial pathogenesis. *Microbiology* 164, 251–259. doi: 10.1099/mic.0.000604
- Dou, Y., Song, F., Guo, F., Zhou, Z., Zhu, C., Xiang, J., et al. (2017). *Acinetobacter baumannii* quorum-sensing signalling molecule induces the expression of drug-resistance genes. *Mol. Med. Rep.* 15, 4061–4068. doi: 10.3892/mmr.2017.6528
- Eijkelkamp, B. A., Begg, S. L., Pederick, V. G., Trapetti, C., Gregory, M. K., Whittall, J. J., et al. (2018). Arachidonic acid stress impacts pneumococcal fatty acid homeostasis. *Front. Microbiol.* 9:813. doi: 10.3389/fmicb.2018.00813
- Erdonmez, D., Rad, A. Y., and Aksoz, N. (2017). Quorum sensing molecules production by nosocomial and soil isolates *Acinetobacter baumannii*. *Arch. Microbiol.* 199, 1325–1334. doi: 10.1007/s00203-017-1408-8
- Fernandez-Garcia, L., Ambroa, A., Blasco, L., Bleriot, I., Lopez, M., Alvarez-Marín, R., et al. (2018). Relationship between the quorum network

(JJKH20170820KJ and JJKH20170852KJ), and grants from the Department of Finance of Jilin Province (SWKYZ002).

## ACKNOWLEDGMENTS

We thank Beijing Genomics Institute (BGI) for assistance with bioinformatics analysis. We appreciate Ayush Kumar from the Department of Microbiology, University of Manitoba, Winnipeg, MB, Canada, for the *A. baumannii* ATCC 17978 strain. We appreciate Mingsheng Dong from Nanjing Agricultural University for the *Chromobacterium violaceum* CV026 strain. We appreciate Mingyong Zeng from Ocean University of China for the *A. tumefaciens* KYC55 and R10 strains. We would also thank the proofreading work of American Journal Experts (AJE) for this manuscript.

## SUPPLEMENTARY MATERIAL

The Supplementary Material for this article can be found online at: <https://www.frontiersin.org/articles/10.3389/fmicb.2021.679241/full#supplementary-material>

- (sensing/quenching) and clinical features of pneumonia and bacteraemia caused by *a. baumannii*. *Front. Microbiol.* 9:3105. doi: 10.3389/fmicb.2018.03105
- Galperin, M. Y., Makarova, K. S., Wolf, Y. I., and Koonin, E. V. (2015). Expanded microbial genome coverage and improved protein family annotation in the COG database. *Nucleic Acids Res.* 43, D261–D269.
- Geisinger, E., and Isberg, R. R. (2015). Antibiotic modulation of capsular exopolysaccharide and virulence in *Acinetobacter baumannii*. *PLoS Pathog.* 11:e1004691. doi: 10.1371/journal.ppat.1004691
- Harding, C. M., Hennon, S. W., and Feldman, M. F. (2018). Uncovering the mechanisms of *Acinetobacter baumannii* virulence. *Nat. Rev. Microbiol.* 16, 91–102. doi: 10.1038/nrmicro.2017.148
- Harris, G., Kuo Lee, R., Lam, C. K., Kanzaki, G., Patel, G. B., Xu, H. H., et al. (2013). A mouse model of *Acinetobacter baumannii*-associated pneumonia using a clinically isolated hypervirulent strain. *Antimicrob. Agents. Chemother.* 57, 3601–3613. doi: 10.1128/aac.00944-13
- Heeb, S., Itoh, Y., Nishijyo, T., Schnider, U., Keel, C., Wade, J., et al. (2000). Small, stable shuttle vectors based on the minimal pVS1 replicon for use in gram-negative, plant-associated bacteria. *Mol. Plant Microbe Interact.* 13, 232–237. doi: 10.1094/mpmi.2000.13.2.232
- Herzog, R., Peschek, N., Frohlich, K. S., Schumacher, K., and Papenfort, K. (2019). Three autoinducer molecules act in concert to control virulence gene expression in *Vibrio cholerae*. *Nucleic Acids Res.* 8, 3171–3183. doi: 10.1093/nar/gky1320
- Howe, E. A., Sinha, R., Schlauch, D., and Quackenbush, J. (2011). RNA-Seq analysis in MeV. *Bioinformatics* 15, 3209–3210. doi: 10.1093/bioinformatics/btr490
- Huerta-Cepas, J., Forslund, K., Coelho, L. P., Szklarczyk, D., Jensen, L. J., von Mering, C., et al. (2017). Fast genome-wide functional annotation through orthology assignment by eggNOG-mapper. *Mol. Biol. Evol.* 1, 2115–2122. doi: 10.1093/molbev/msx148
- Jiang, J. H., Hassan, K. A., Begg, S. L., Rupasinghe, T. W. T., Naidu, V., Pederick, V. G., et al. (2019). Identification of novel *Acinetobacter baumannii* host fatty acid stress adaptation strategies. *mBio* 5:10.
- Kaiser, J. C., Sen, S., Sinha, A., Wilkinson, B. J., and Heinrichs, D. E. (2016). The role of two branched-chain amino acid transporters in *Staphylococcus aureus* growth, membrane fatty acid composition and virulence. *Mol. Microbiol.* 102, 850–864. doi: 10.1111/mmi.13495

- Kaplan, J. B., Izano, E. A., Gopal, P., Karwacki, M. T., Kim, S., Bose, J. L., et al. (2012). Low levels of beta-lactam antibiotics induce extracellular DNA release and biofilm formation in *Staphylococcus aureus*. *mBio* 3, e198–e112.
- Kim, G. L., Lee, S., Luong, T. T., Nguyen, C. T., Park, S. S., Pyo, S., et al. (2017). Effect of decreased BCAA synthesis through disruption of *ilvC* gene on the virulence of *Streptococcus pneumoniae*. *Arch. Pharm. Res.* 40, 921–932. doi: 10.1007/s12272-017-0931-0
- Kim, M. K., Zhao, A., Wang, A., Brown, Z. Z., Muir, T. W., Stone, H. A., et al. (2017). Surface-attached molecules control *Staphylococcus aureus* quorum sensing and biofilm development. *Nat. Microbiol.* 22:17080.
- King, L. B., Pangburn, M. K., and McDaniel, L. S. (2013). Serine protease PKF of *Acinetobacter baumannii* results in serum resistance and suppression of biofilm formation. *J. Infect. Dis.* 207, 1128–1134. doi: 10.1093/infdis/jis939
- Lade, H., Paul, D., and Kweon, J. H. (2014). Isolation and molecular characterization of bioforming bacteria and profiling of quorum sensing signal molecules from membrane bioreactor activated sludge. *Int. J. Mol. Sci.* 4, 2255–2273. doi: 10.3390/ijms15022255
- Law, R. J., Hamlin, J. N., Sivro, A., McCorrister, S. J., Cardama, G. A., and Cardona, S. T. (2008). A functional phenylacetic acid catabolic pathway is required for full pathogenicity of *Burkholderia cenocepacia* in the *Caenorhabditis elegans* host model. *J. Bacteriol.* 190, 7209–7218. doi: 10.1128/jb.00481-08
- Li, H., Li, X., Song, C., Zhang, Y., Wang, Z., Liu, Z., et al. (2017). Autoinducer-2 facilitates *Pseudomonas aeruginosa* PAO1 pathogenicity in vitro and in vivo. *Front. Microbiol.* 8:1944. doi: 10.3389/fmicb.2017.01944
- Li, X., Li, J., Hu, X., Huang, L., Xiao, J., Chan, J., et al. (2015). Differential roles of the hemerythrin-like proteins of *Mycobacterium smegmatis* in hydrogen peroxide and erythromycin susceptibility. *Sci. Rep.* 26, 16130.
- Liu, D., Liu, Z. S., Hu, P., Cai, L., Fu, B. Q., Li, Y. S., et al. (2016). Characterization of surface antigen protein 1 (SurA1) from *Acinetobacter baumannii* and its role in virulence and fitness. *Vet. Microbiol.* 15, 126–138. doi: 10.1016/j.vetmic.2016.02.018
- Miller, M. B., and Bassler, B. L. (2001). Quorum sensing in bacteria. *Ann. Rev. Microbiol.* 55, 165–199.
- Minato, Y., Fassio, S. R., Wolfe, A. J., and Hase, C. C. (2013). Central metabolism controls transcription of a virulence gene regulator in *Vibrio cholerae*. *Microbiology* 159, 792–802. doi: 10.1099/mic.0.064865-0
- Mukherjee, S., Moustafa, D. A., Stergioula, V., Smith, C. D., Goldberg, J. B., and Bassler, B. L. (2018). The PqsE and RhlR proteins are an autoinducer synthase-receptor pair that control virulence and biofilm development in *Pseudomonas aeruginosa*. *Proc. Natl. Acad. Sci. U.S.A.* 2, E9411–E9418.
- Mukhopadhyay, S., Nair, S., and Ghosh, S. (2012). Pathogenesis in tuberculosis: transcriptomic approaches to unraveling virulence mechanisms and finding new drug targets. *FEMS Microbiol. Rev.* 36, 463–485. doi: 10.1111/j.1574-6976.2011.00302.x
- Niu, C., Clemmer, K. M., Bonomo, R. A., and Rather, P. N. (2008). Isolation and characterization of an autoinducer synthase from *Acinetobacter baumannii*. *J. Bacteriol.* 190, 3386–3392. doi: 10.1128/jb.01929-07
- Peleg, A. Y., Jara, S., Monga, D., Eliopoulos, G. M., Moellering, R. C. Jr., and Mylonakis, E. (2009). *Galleria mellonella* as a model system to study *Acinetobacter baumannii* pathogenesis and therapeutics. *Antimicrob. Agents Chemother.* 53, 2605–2609. doi: 10.1128/aac.01533-08
- Pereira-Dutra, F. S., Teixeira, L., de Souza Costa, M. F., and Bozza, P. T. (2019). Fat, fight, and beyond: the multiple roles of lipid droplets in infections and inflammation. *J. Leukoc. Biol.* 106, 563–580. doi: 10.1002/jlb.4mr0119-035r
- Rameshwaram, N. R., Singh, P., Ghosh, S., and Mukhopadhyay, S. (2018). Lipid metabolism and intracellular bacterial virulence: key to next-generation therapeutics. *Future Microbiol.* 13, 1301–1328. doi: 10.2217/fmb-2018-0013
- Rutherford, S. T., and Bassler, B. L. (2012). Bacterial quorum sensing: its role in virulence and possibilities for its control. *Cold Spring Harb. Perspect. Med.* 1:2.
- Smani, Y., Dominguez-Herrera, J., and Pachon, J. (2013). Association of the outer membrane protein Omp33 with fitness and virulence of *Acinetobacter baumannii*. *J. Infect. Dis.* 15, 1561–1570. doi: 10.1093/infdis/jit386
- Smith, M. G., Gianoulis, T. A., Pukatzki, S., Mekalanos, J. J., Ornston, L. N., Gerstein, M., et al. (2007). New insights into *Acinetobacter baumannii* pathogenesis revealed by high-density pyrosequencing and transposon mutagenesis. *Genes Dev.* 1, 601–614. doi: 10.1101/gad.1510307
- Stacy, D. M., Welsh, M. A., Rather, P. N., and Blackwell, H. E. (2012). Attenuation of quorum sensing in the pathogen *Acinetobacter baumannii* using non-native N-Acyl homoserine lactones. *ACS Chem. Biol.* 19, 1719–1728.
- Tang, J., Chen, Y., Wang, X., Ding, Y., Sun, X., and Ni, Z. (2020). Contribution of the AbaI/AbaR quorum sensing system to resistance and virulence of *Acinetobacter baumannii* clinical strains. *Infect. Drug Resist.* 13, 4273–4281. doi: 10.2147/idr.s276970
- Tang, J., Zhu, H., Cai, L., Tang, T., Tang, J., Sun, Y., et al. (2018). Postoperative infection caused by *Acinetobacter baumannii* misdiagnosed as a free-living amoeba species in a humeral head hemiarthroplasty patient: a case report. *Infect. Dis. Poverty.* 31:33.
- Tatusov, R. L., Galperin, M. Y., Natale, D. A., and Koonin, E. V. (2000). The COG database: a tool for genome-scale analysis of protein functions and evolution. *Nucleic Acids Res.* 1, 33–36. doi: 10.1093/nar/28.1.33
- Teufel, R., Mascaraque, V., Ismail, W., Voss, M., Perera, J., Eisenreich, W., et al. (2010). Bacterial phenylalanine and phenylacetate catabolic pathway revealed. *Proc. Nat. Acad. Sci. U.S.A.* 10, 14390–14395. doi: 10.1073/pnas.1005399107
- Tomaras, A. P., Dorsey, C. W., Edelmann, R. E., and Actis, L. A. (2003). Attachment to and biofilm formation on abiotic surfaces by *Acinetobacter baumannii*: involvement of a novel chaperone-usher pili assembly system. *Microbiology* 149, 3473–3484. doi: 10.1099/mic.0.26541-0
- Vila-Farres, X., Parra-Millan, R., Sanchez-Encinales, V., Varese, M., Ayerbe-Algaba, R., Bayo, N., et al. (2017). Combating virulence of gram-negative bacilli by ompa inhibition. *Sci. Rep.* 31:14683.
- Wang, N., Ozer, E. A., Mandel, M. J., and Hauser, A. R. (2014). Genome-wide identification of *Acinetobacter baumannii* genes necessary for persistence in the lung. *mBio* 3, e1163–e1114.
- Wong, D., Nielsen, T. B., Bonomo, R. A., Pantapalangkoor, P., Luna, B., and Spellberg, B. (2017). Clinical and pathophysiological overview of acinetobacter infections: a century of challenges. *Clin. Microbiol. Rev.* 30, 409–447. doi: 10.1128/cmr.00058-16
- Xie, Y., Shao, X., Zhang, Y., Liu, J., Wang, T., Zhang, W., et al. (2019). *Pseudomonas savastanoi* two-component system rhprs switches between virulence and metabolism by tuning phosphorylation state and sensing nutritional conditions. *mBio* 19:10.
- Yanjun, S., Shuixiu, L., Yajing, Z., Yishan, Z., Yan, L., Yuanying, J., et al. (2019). ADH1 promotes *Candida albicans* pathogenicity by stimulating oxidative phosphorylation. *Int. J. Med. Microbiol.* 309:151330. doi: 10.1016/j.ijmm.2019.151330
- Yu, G., Wang, L. G., Han, Y., and He, Q. Y. (2012). clusterProfiler: an R package for comparing biological themes among gene clusters. *OMICS* 16, 284–287. doi: 10.1089/omi.2011.0118
- Yu, Z., Zhu, Y., Fu, J., Qiu, J., and Yin, J. (2019). Enhanced NADH metabolism involves colistin-induced killing of *Bacillus subtilis* and *Paenibacillus polymyxa*. *Molecules* 22, 24.
- Zuo, J., Yin, H., Hu, J., Miao, J., Chen, Z., Qi, K., et al. (2019). Lsr operon is associated with AI-2 transfer and pathogenicity in avian pathogenic *Escherichia coli*. *Vet. Res.* 12:109.

**Conflict of Interest:** The authors declare that the research was conducted in the absence of any commercial or financial relationships that could be construed as a potential conflict of interest.

Copyright © 2021 Sun, Ni, Tang, Ding, Wang and Li. This is an open-access article distributed under the terms of the Creative Commons Attribution License (CC BY). The use, distribution or reproduction in other forums is permitted, provided the original author(s) and the copyright owner(s) are credited and that the original publication in this journal is cited, in accordance with accepted academic practice. No use, distribution or reproduction is permitted which does not comply with these terms.